

Systematic approach to find a suitable floating PV-structure on a given location

Comparing the environmental loads on different types of floating solar structures

N. Wemekamp



Master
Offshore Engineering

Delft University of Technology,

October 2, 2023

Author: N. Wemekamp
Supervisor TU Delft: Dr. O. Colomes Gené
Dr. S. Agarwal
Supervisor Ventolines: Ir. M. Klap

Abstract

The Netherlands has agreed, by signing the Paris Agreement, to be climate-neutral by 2050. To reach this goal, many large-scale renewable energy projects need to be developed in the coming years using for example wind, geothermal or solar energy. The problem with these projects is that they require large amounts of land and are especially needed in densely populated areas where the energy demand is high. For solar energy, a solution is to move it to bodies of water, creating a floating photovoltaic (FPV) system. Besides not requiring valuable land, FPV offers other benefits; The water has a cooling effect on the panels, increasing the efficiency of the solar panels. There is less water evaporation, which is desired in for example drink water basins. FPV systems have a high potential for system integration with nearshore and offshore wind turbines, optimizing space utilization and making cable pooling possible.

Multiple companies have already developed an FPV system, each designed for specific water categories and having its own (dis-)advantages. This thesis analyses different types of FPV systems and offers a tool for project developers to help decide what kind of system to select in a preliminary phase of project development.

As input to this decision tool, the environmental loads acting on FPV systems are calculated. The forces due to the wind, current and waves are found for three different types of systems. These systems are *Floating Solar*, Zimfloat and OceanSun. The forces are first found on a small section of the structures and then scaled up to a size of one hectare including sheltering factors. The results show that the membrane-type structure of OceanSun has significantly lower environmental forces than the *Floating Solar* and Zimfloat systems. These two are both built up of high-density polyethylene floaters and a metal frame holding the PV panels. The wind force is the highest on the *Floating solar* structure due to the larger tilt angle. The wave forces are found to be the highest for the Zimfloat structure which can be explained by the floaters. These are square blocks instead of circular tubes, making them less aerodynamic and having a larger volume which increases the inertia forces.

The decision tool uses a multi-criteria analysis that takes twelve important aspects of an FPV system into account including the environmental loads. Examples of these criteria are energy production, costs, energy density and also less quantifiable criteria such as ecological impact, safety and the technical readiness level of the systems. The tool compares six different types of systems and can easily be adjusted to a specific location by changing the weight factors. With these weight factors, the tool provides a clear overview of the most important aspects of an FPV system and helps to decide in an early phase of project development whether a system is suitable for the desired location or not.

The decision tool is used for the case study 'Haringvliet'. Haringvliet is a former estuary in the Netherlands and is chosen as a potential location for an FPV park. The calculations mentioned above are performed using the site conditions found at Haringvliet. The conclusion of the decision tool is that the structure of *Floating Solar* is the most suitable for the Haringvliet. This is partly because Haringvliet is an ecologically protected area and the floating solar structure is very open, letting sunlight pass through the system into the water.

Acknowledgements

This thesis marks the end of my time at the TU Delft. I really enjoyed living and studying in Delft and want to thank everyone who has been a part of this journey. All the activities next to my study, such as rowing at Proteus, made these years unforgettable and helped me to stay motivated. I want to thank Mathijs for the moral support during the last months of my thesis at lunch and coffee breaks. Thanks to Folkert for proofreading and giving feedback on my report. And of course, thanks to Hanna for her support during my work and needed distractions after some long days.

I want to thank the entire team of Ventolines for the opportunity to be an intern and for their support and interest in my graduation. Special thanks to Maarten Klap for his daily guidance, including interesting discussions and motivation. And thanks to my fellow interns at Ventolines for their support during the intern meetings.

I want to thank the committee members Oriol Colomes Gené as chairman and Shagun Agarwal for their guidance in the process and their useful feedback on my methods and results.

Lastly, I want to thank Ralph van Dijk and Henko Engberts from the company Floating Solar, Petter Grøn from OceanSun and William Otto from Marin. Meeting with these people helped me gain insides into the upcoming floating solar industry.

Nebo Wemekamp
October 2023, Delft

Notation & Abbreviations

Notation	Description	Unit
ρ_A	Density of air	$\frac{kg}{m^3}$
ρ_W	Density of water	$\frac{kg}{m^3}$
F_w	Wind load	N
U_{10}	Wind velocity at 10m	$\frac{m}{s}$
C_D	Drag coefficient	-
C_L	Lift coefficient	-
C_m	Inertia coefficient	-
C_a	Added mass coefficient	-
A	Projected area	m^2
T	Wave period	s
H	Wave height	m
H_s	Significant wave height	m
a	Amplitude of wave	m
L	Wave length	m
f_p	Peak frequency	rad
F	Fetch	m
g	Gravitational constant	$\frac{m}{s^2}$
h or d	Water depth	m
ω	Wave frequency	s^{-1}
k	Wave number	m^{-1}
S	Shielding factor	-
ν	kinematic viscosity	$\frac{m^2}{s}$
θ	Tilt angle	$^\circ$
Ha	Hectare	m^2
a	Scale factor	-

Abbreviation	Description
FPV	Floating photovoltaic
HDPE	High density Polyethylene
KNMI	Koninklijk Nederlands Meteorologisch Instituut
MCA	Multi Criteria Analyses
TRL	Technical Readiness Level
Wp	Watt-peak
Re	Reynolds number
CDBT	Center distance between tubes
Capex	Capital expenditures

Contents

Abstract	i
Acknowledgements	ii
Notation & Abbreviations	iii
1 Introduction	1
1.1 Growth of FPV	2
1.2 Scope of thesis	2
1.3 Outline	2
2 Recap on literature study	3
2.1 Existing floating solar designs	3
2.1.1 Typical FPV structure	3
2.1.2 Structures that are analysed	4
2.2 Design factors of a FPV-park	6
3 Environmental loads	10
3.1 Wind forces	10
3.2 Current forces	12
3.3 Wave forces	12
3.3.1 Wave model	13
3.3.2 Morison equations	14
4 Calculations on existing structures.	16
4.1 Assumptions for calculations	16
4.2 Input parameters	17
4.3 Method for calculations	18
4.4 <i>Floating Solar</i> (Company)	20
4.4.1 Wind force	20
4.4.2 Current force	21
4.4.3 Wave force	22
4.4.4 Waves + current	23
4.4.5 Overview of the forces	24
4.5 Ocean Sun, flexible membrane	24
4.5.1 Wind force	25
4.5.2 Current force	26
4.5.3 Wave force	26
4.6 ZimFloat	29
4.6.1 Wind force	30
4.6.2 Current force	30
4.6.3 Wave force	30
4.7 Overview of environmental loads	31
5 Multi-Criteria Analyses (MCA)	33
5.1 Criteria:	33
5.2 Weight factor	35
5.2.1 How to determine the weight factors	35
5.3 Deal breakers	36
5.4 MCA without a location	36

6	Case study: Haringvliet	39
6.1	Introduction	39
6.2	Site conditions:	39
6.2.1	Location	39
6.2.2	Wind	40
6.2.3	Bathymetry	42
6.2.4	Soil composition	42
6.2.5	Waves	43
6.2.6	Tides	46
6.2.7	Current.	46
6.2.8	Natura 2000.	46
6.3	Decision matrix.	46
6.3.1	Weight factors.	46
6.3.2	Filled in matrix	47
6.3.3	Results	49
7	Discussion	50
7.1	Environmental loads	50
7.2	Multi criteria matrix	51
7.3	Case study Haringvliet.	51
8	Conclusions	52
9	Recommendations	54
9.1	For future research	54
9.2	For Ventolines.	54
	Bibliography	55
	Appendices	58
A	Appendix A	59
B	Appendix B	61
C	Appendix C	65

1

Introduction

There is an increasing demand for renewable energy to reach climate goals set in the Paris climate agreement. The EU members agreed that the greenhouse emissions should be lowered by a minimum of 55% in 2030 and want to be climate-neutral by 2050 [1]. In order to achieve this goal the Dutch government set targets for the production of renewable energy. In 2030 this should be at least 27% and in 2050 almost all energy should be renewable [2]. In 2022 only 15% of all energy used in the Netherlands came from renewable sources [3].

To reach these climate goals new renewable energy projects need to be developed in the coming years. A part of these projects will harvest energy from the wind with new offshore wind parks that are already planned such as Hollandse Kust and IJmuiden Ver [4]. Another part will use geothermal energy that uses the heat of the earth at a depth of more than 500 meters which should provide heat to 2.2 million Dutch households by 2030 [5]. A part of the renewable energy will use energy from the sun. Solar energy can be generated using photovoltaic (PV) systems. This technology is already widely used with solar panels located on rooftops and large ground-mounted solar parks on fields. Solar energy has multiple advantages, it is relatively low costs, it is reliable with a minimum level of maintenance and it can be easily scaled up [6].

The problem however with these solar parks is that they require a relatively large area and take up land that is normally used for housing, agriculture or nature [7]. Especially in highly populated areas where the demand for energy is high, covering only rooftops with many high-rise buildings is insufficient and land for ground-based solar can be very expensive or even unavailable. Approximately 50% of the world's population lives near a surface of freshwater [8]. A solution is to move solar panels to unused water areas and create floating solar panels, also known as floating photovoltaic (FPV) systems. These FPV systems can be installed on bodies of water such as lakes, reservoirs and the ocean. The opportunity for FPV is very large and can have a major contribution in the transition towards a world that is fully powered by renewable energy.

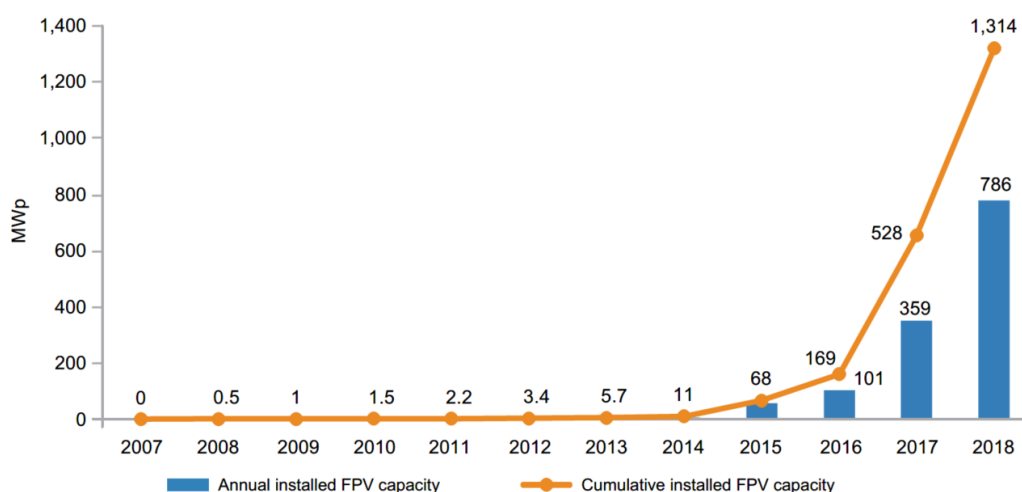


Figure 1.1: Global installed FPV capacity [9]

1.1. Growth of FPV

The first floating solar system is from 2007, the project is called Aichi and is done by the National Institute of Advanced Science and Technology in Japan. The first significant grid-connected system was installed by a winery called Far Niente in California in 2008 [10]. The winery wanted to generate solar power without sacrificing land for the vines and therefore installed FPV on the vineyard irrigation pond. Since then many companies in different countries started research on and the development of FPV systems. In the first years, only small pilot projects were installed and from 2015 the installed capacity grew rapidly as can be seen in Figure 1.1. In 2018 73% of the global installed FPV capacity (1.3 GWp) was located in China [9]. Jin et al. [11] estimated the global potential for FPV to be over 9000 TWh per year. In their research, they analysed 114555 suitable reservoirs (larger than 0.01km^2) for FPV and assumed a coverage of 30% and a maximum size of 30km^2 per FPV system.

1.2. Scope of thesis

The goal of this thesis is to find a systematic method to determine what kind of floating PV structure is the most suitable for a given location. This is achieved by answering the research questions below. The lies in the rougher inland waters in the Netherlands, however, the method is also useful for calmer waters or offshore locations. This method will then be used in a case study to find which technology is the most suitable at location Haringvliet.

Main research question:

How to determine which floating-PV technology to select for a specific location in a preliminary phase of project development?

Sub-question 1:

Which criteria are the most important for the selection of a floating-PV structure?

Sub-question 2:

What are the wind, waves and current loads on different FPV structures?

Sub-question 3: (Case study)

Which existing floating PV structure is the most suitable for the rougher inland water conditions at Haringvliet?

Sub-question 3a

What are the environmental site conditions for the Haringvliet location?

1.3. Outline

This thesis will start with a recap of the literature study including the background on floating PV structures and the design factors. Then in chapter 3 the environmental loads that act on an FPV structure are presented and in chapter 4 these loads are found for three different types of FPV structures. In chapter 5 a systematic method is introduced to select an FPV structure for a desired location. This method is then used in the case study presented in chapter 6. In the end a discussion (chapter 7) and a conclusion (chapter 8) are given together with recommendations for future work.

2

Recap on literature study

In this chapter, the background information needed to understand the methods used in this thesis is presented. In [subsection 2.1.1](#) a typical FPV structure is presented and an overview of different available FPV structures is given. Then the basic principle of the structures that will be analysed in this thesis is explained. In [section 2.2](#) different aspects are presented that have an influence on the design of an FPV structure.

2.1. Existing floating solar designs

2.1.1. Typical FPV structure

There are many different existing concepts for an FPV system. They can differ in the type of floater, usage of a subframe, height of the deck and rigidity of the total structure [12]. However, the underlining bases are often very similar and an example of a typical layout can be seen in [Figure 2.1](#). The most important components are the PV module, the floater, the frame, a mooring system, anchors and the electrical infrastructure including transformers, power inverters and cables. The frame, usually made of galvanized steel or aluminium, provides a rigid surface for PV-modules placement, while the mooring system attaches the floaters to anchors and keeps the structure in place.

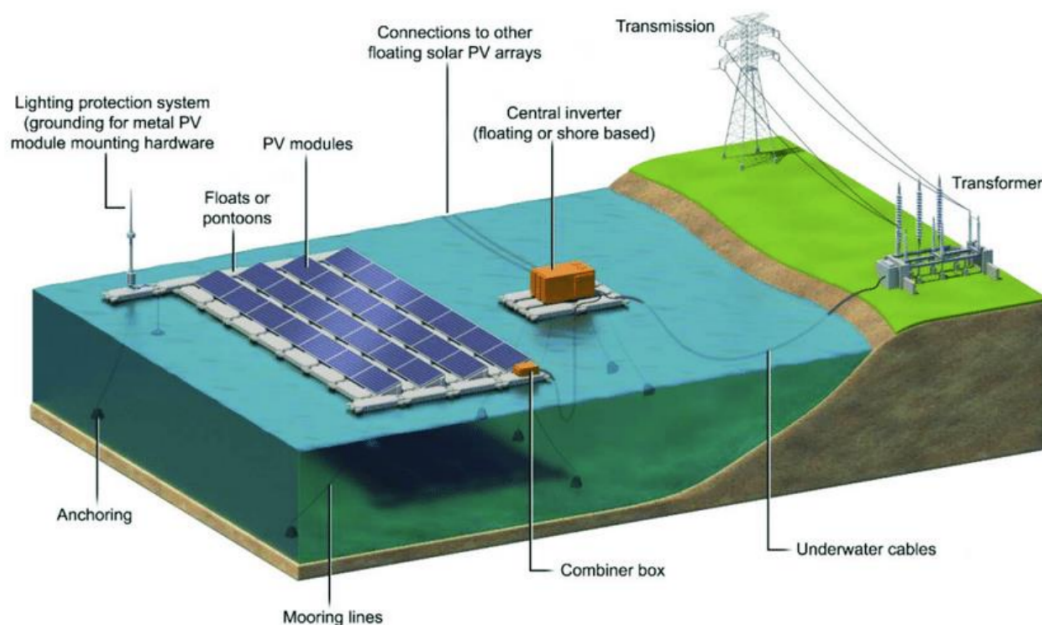


Figure 2.1: Overview of a typical FPV-system [13]

There are multiple companies and research institutions developing and testing different concepts and technologies for floating solar [12]. What all designs have in common is that the floater must be able to hold a PV panel and can withstand environmental forces. However, the differences between the technologies can be very high. The structures can differ in the materials, shape of floaters, flexibility

and size and are designed for specific site conditions. In [Figure 2.2](#) a schematic overview of different FPV categories is given. In the bottom (light-blue) boxes examples of companies with designs in those categories are given. The left-most companies have relatively simple designs and are already widely used [[14](#)][[15](#)], moving to the right the systems are more complex and often still in the development phase [[16](#)][[17](#)][[18](#)].

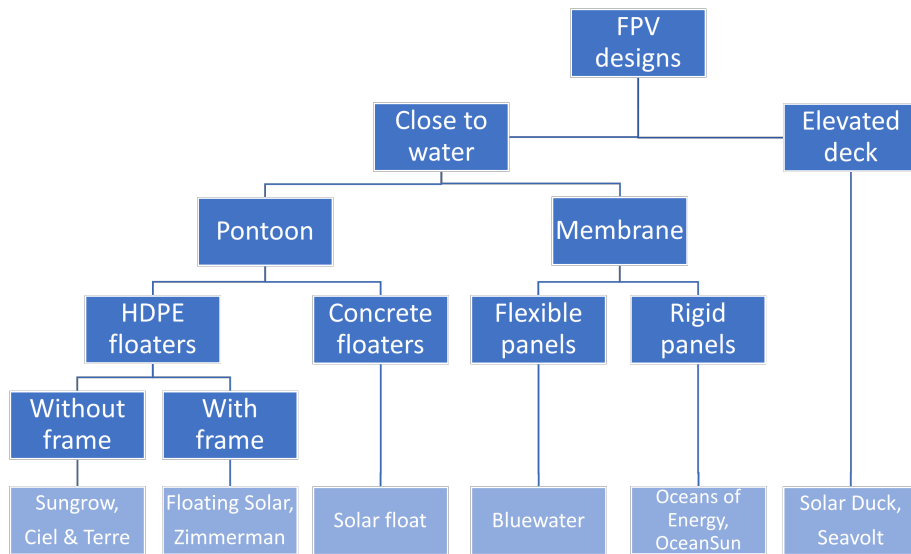


Figure 2.2: Overview FPV designs

2.1.2. Structures that are analysed

In the overview provided in [Figure 2.2](#) there are ten different kinds of FPV structures. Not all of these structures are analysed in the scope of this thesis. Some are still in a very early stage of development such as Bluewater and Seavolt and are therefore left out. Ciel & Terre and Sungrow have a very similar design and therefore the decision is made to only analyse the structure of Ciel & Terre of these two. The reason for this choice is that it is easier to work with a European than an Asian supplier regarding the needed certificates for installing an FPV park. The remaining six systems are analysed and the basic concept of each system is explained below.

Ciel & Terre

The first structure is from the French company Ciel & Terre [[14](#)]. A close-up of their structure, called Hydrelío, can be seen in [Figure 2.3](#). They use a pontoon made from high-density polyethylene (HDPE) which is lightweight and has a high buoyancy to support the solar panels. Usually, 1 pontoon or main float holds 1 PV panel and secondary floats can be added for walkways. The pontoon is specially designed so the panels can be mounted directly including an optional tilt angle. These pontoons can be orientated in both South of East-West positions. These types of floaters are mainly used in calm waters with mild wind- and wave conditions and are typically found on inland water basins.

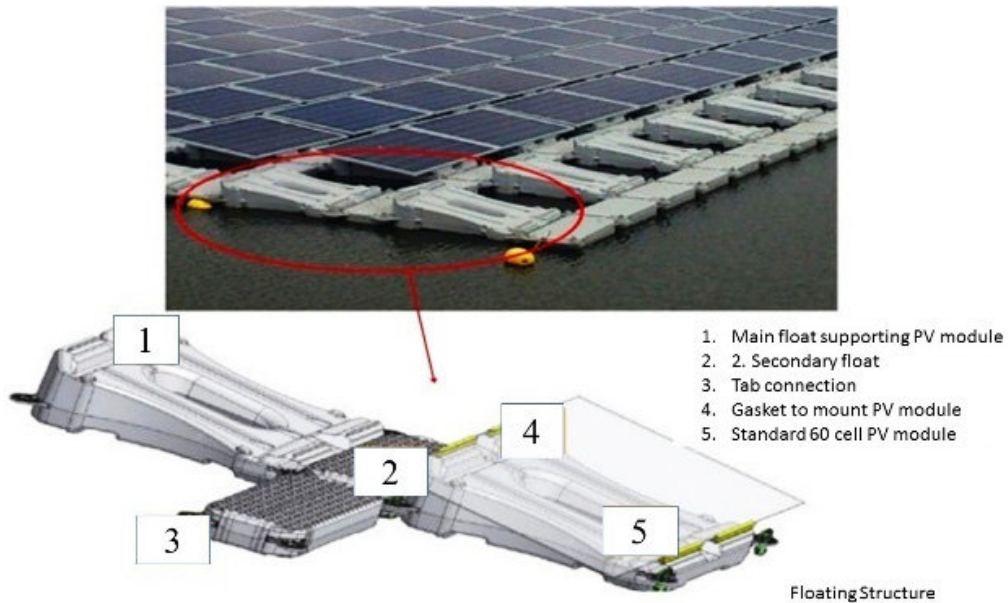


Figure 2.3: HDPE pontoon from Ciel et Terre [12]

ZimFloat

In the design of Zimmermann [19], called ZimFloat, multiple PV panels are placed on what they call boats. One boat consists of 4 HDPE floaters with a metal frame that supports 2 rows of PV panels. One boat can hold 12, 16 or 18 PV panels to meet the design requirements per project. These boats can be placed in long rows and multiple rows from the entire FPV farm. Between each boat, there is a gap for sunlight to reach the water to preserve the underwater life.

Floating Solar

The name of *Floating Solar* is printed in italics in this thesis to avoid confusion with the term Floating solar. The structure from *Floating Solar* is built up from sealed plastic tubes as floaters and coated steel frames on which the panels are placed. Multiple tubes are connected to create a large circular structure. The structure uses few materials and is easy to assemble. This structure can withstand relatively high wind and waves and is successfully tested with a three-year trial on the Slufter near the Maasvlakte [20]. *Floating Solar* specialises in its optimal solar tracking technology. With this technology the circular islands rotate, changing the azimuth-angle, so that the solar panels are in the optimal position all day and rotate back during the night. The energy it costs to rotate the islands is much less than the extra energy production [21].



Figure 2.4: ZimFloat boat with multiple PV-panels [19]



Figure 2.5: Floating Solar sealed plastic tubes [21]

Oceans of Energy

In the concept by Oceans of Energy, the structure floats just above the water and the standard rigid solar panels lay flat on the surface. Oceans of Energy has an operating and grid-connected test site in the North Sea, that survived multiple storms and is now being scaled up to 1MW. The system is

designed to withstand waves up to 14m [16]. A challenge for this structure is that it is very inviting for birds and that bird-dropping can limit energy production over time.



Figure 2.6: Oceans of Energy [16]

OceanSun

OceanSun has a concept that differs from the other membrane concepts because they use buoyancy rings as floaters. The buoyancy rings are two airtight rings placed next to each other made from HDPE. The large circular membrane is supported by these buoyancy rings. This concept has a very low material usage which lowers the production costs [22]. The membrane is even capable of supporting construction workers to walk over the PV panels which makes installation fast and easy.

SolarDuck

SolarDuck is a Dutch company and their concept has a stiff triangular shape with three large vertical cylindrical floaters so the platform is elevated well above the waterline. This structure, designed for offshore conditions, can withstand large waves ($H_s > 5\text{m}$) and high wind speeds ($V > 30\text{m/s}$) [17]. Multiple triangles can be linked together to create a larger floating solar park. The structure is very robust which results in higher production and installation costs than the standard pontoon-type structures.



Figure 2.7: SolarDuck [17]



Figure 2.8: OceanSun [22]

2.2. Design factors of a FPV-park

In this section the different aspects are presented that have an influence on the design of an FPV structure. These design factors are the environmental loads and other aspects that have to be taken into account when designing or selecting an FPV structure.

Wind

The wind load is expected to be one of the highest loads on the structure. The area on which the wind can act is directly related to the load. Large surfaces above water result in higher wind loads. The windspeed increases exponentially with the height above mean water level, therefore a higher structure will have a higher wind load than structures that remain close to the water.

Waves

Waves can result in very large forces on the floating structure if they are present. Important factors contributing to the height of the wave load are the draft, size, shape and rigidity of the structure. A high draft and large underwater volumes will result in larger drag and inertia forces. Very stiff structures such as the Solar Duck concept result in low oscillations. Flexible membranes are designed to move along the waves [23].

Current

Structures with a large underwater area will have a larger drag force due to the currents. Small ponds or lakes will have a very low or no current at all. Rivers, large lakes and offshore locations will have higher currents.

Self cleaning

In order for the solar panels to produce energy the surface has to remain clear of anything that can block the sunlight. A common problem for FPV systems is the accumulation of bird droppings. Panels that are installed at an angle (tilt angle) have a self-cleaning effect. Due to this angle, the panels will be rinsed when it is raining. Note that this only works well in locations where it often rains and will work less in very dry areas. Horizontal-orientated panels without a tilt angle do not have this effect and need to be cleaned in another way. Cleaning can be done manually or with the use of cleaning robots.

Ecology

The ecological effects of an FPV structure on marine life are highly correlated to the amount of sunlight that is able to still reach the water's surface. This can be calculated using the cover ratio. The cover ratio is the ratio between the total water surface and the area that is covered by the structure. For water basins in warm countries, it can be useful to have a high cover ratio to reduce algae growth and limit water evaporation. For locations in an ecologically protected area, such as the Natura 2000 areas in the Netherlands, it is required to let enough sunlight reach the water. Flexible membranes usually have a cover ratio of 1 (completely covered) per island, however, when designing a large FPV park open areas can be created between multiple floaters to allow sunlight to reach the water. The water depth is an important input parameter for the ecological impact of an FPV park. A study commissioned by Ventolines and performed by Witteveen+Bos shows that a high cover ratio and a high water depth both have a negative influence on the presence of water plants. Water plants are not present when the water depth is more than four meters or when the cover ratio is higher than 80%.

Technical Readiness Level (TRL)

The Technical Readiness Level is a method that describes in what phase a technology or system is. A low TRL means that there is only a design. Medium levels are already in the testing or experimenting phase with pilot projects. High levels are structures that already have (multiple) fully commissioned projects. These structures have proven to be stable and safe and can handle the environmental loads. Structures with a low TRL have a higher risk because there is no proven track record and can still have some start-up problems, high TRL structures are often improved and optimised for the best results and lower costs.

Safety

As for all structures on water, safety is a very important factor. The combination of water and electricity can be dangerous. Even if the system is well designed it will be necessary to access the structure to inspect, clean or perform other types of maintenance. Therefore it is needed to safely get to and walk over the structure. There are many measurements that can be taken to improve the safety of the structure. It should be easy to get to the structure (by boat) and rigid walkways should provide stable access to all panels for multiple workers including heavy machinery or spare parts. Therefore access buoyancy of the floaters is needed to handle this extra load. Safety railings, cable protection or other risk mitigation will improve the overall safety of an FPV structure.

Maintenance

During operations, it will be necessary to perform inspections and maintenance when needed. If for any reason a floater, panel, connection piece or mooring line fails it should be easily replaceable. Therefore it is important that the entire system is easily accessible for maintenance workers and that spare parts are easily available. Maintenance can be divided into four categories: Preventive, predictive, corrective, and exceptional. Preventive maintenance is for example visual inspections on the floaters,

panels and mooring lines. Predictive are for example the cleaning of the panels when performance losses are measured. Corrective maintenance is done after an incident or problem is noted and will require repairing or replacing parts. The last category is exceptional maintenance, and this is done after a major unexpected incident that can result in long downtime and sometimes even the need to bring a part of the FPV structure back to shore. A modular build system that uses standard available PV panels is easier to maintain. Sun tracking systems have moving parts that result in a higher chance of failure and can increase the need for maintenance.

Installation

The installation of the FPV park can be a difficult task that is highly dependent on the site conditions. Some systems are only available in standard shapes and/or sizes while other systems can easily be adjusted to the shape and size of the site. The construction and installation of the FPV system can in most cases be done on land nearby for inland or nearshore locations. For large (Offshore) systems it is sometimes needed to build the system at another location and then be transported to the desired location by large vessels. It is beneficial if the required parts are of standard sizes and therefore locally available. Furthermore, the usage of recyclable materials will make decommissioning easier and is better for the environment.

Energy density

The main goal of the FPV system is of course to generate renewable electricity in an efficient way, producing as much energy as possible per area. The energy density depends on the type of PV panels and the spacing between the panels. If specialised (flexible) panels are used the capacity or efficiency of these specialised panels can be lower than that of the standard PV panels. The current maximum energy density is approximately 2MPw/Ha using standard mono-crystalline panels (400Wp with an area of $2m^2$). This is achieved when the panels are placed flat without any space in between the panels. The energy density in (MWp/Ha) can be found by dividing the installed capacity (in MWp) by the total area needed (in Ha). Flexible membranes or other flat systems have a significantly high energy density because there is almost no space needed between the solar panels. Note that the highest energy density does not directly mean that the system will produce the most energy.

Full load hours

The layout and orientation w.r.t. the sun influences the number of hours the sun reaches the panels effectively. This efficiency is found by the number of hours per year that the system delivers the rated capacity also known as full load hours. It is calculated by dividing the expected generated electricity (in kWh/year) by the installed capacity (in kWp). The optimal orientation for a solar panel in the northern hemisphere is directed to the south with a tilt angle that is dependent on the latitude and is around 20 degrees for northern Europe. An orientation in the East-West direction results in lower radiation and a more evenly distributed energy yield per day. Some systems are equipped with a sun tracking system that rotates the panels over 1 or sometimes even 2 axes to achieve an even higher energy yield per installed capacity. This extra movement will cost only a small part of the extra generated energy [21]. Note that the full load hours are in first place determined by the location of the FPV system and thereby the radiation of the sun. However, for the comparison of the different systems the radiation is a constant factor. Flat horizontal panels have a relatively low number of full load hours, tilted panels with an East-West orientation will perform better than tilted panels facing South and the highest full load hours are found for single and double-axis sun tracking systems.

Capital Expenditures (CAPEX)

The price of the FPV farm has to be earned back by selling the generated electricity. Therefore it is important to construct a system that is capable of withstanding all the loads and has a high energy yield but is not too expensive to build and install. Small and light systems can be much cheaper than large over-designed structures due to material and transportation costs. The costs of the system itself and known as capital expenditures (CAPEX). These prices are given in euros per installed capacity (EUR/Wp).

Anchoring and mooring

The anchoring and mooring system keeps the structure in place and is a crucial part of an FPV system. Deciding what kind of mooring system to install is extremely site-specific, and depends on the depth, the soil, water level variations, whether bank anchoring is possible and more site-specific demands. The anchoring and mooring selection itself requires an extra detailed study after a system is chosen for a location.

Ice and snow

When designing a FPV system it is important to determine the additional loads of snow and ice if freezing temperatures are common at the site. Snowfall can lead to an increase in weight, especially for flat surfaces, and thereby lowering the elevation of the panels. Snow load can be estimated using the Eurocode and is location-dependent. For the Netherlands, a snow load of $0.2 \frac{kN}{m^2}$ with peaks in the north and region Rotterdam of $0.4 \frac{kN}{m^2}$ are expected with a return period of 50 years [24]. Additional buoyancy is needed to handle the extra weight and prevent damage to the panels or failure at the floaters. Most FPV structures are capable of handling freezing temperatures and even frozen water. However, a problem can occur when ice floes get into a drift due to the wind. This can result in very high forces in the mooring lines or on the floaters when the ice hits the FPV system.

3

Environmental loads

The most important loads on the structures are the wind, current and waves loads see [Figure 3.1](#). The wind will act on the part of the structure that is above the waterline and the waves and current will act on the submerged part of the structure. How these loads can be calculated will be discussed in this chapter. For this research it is not needed to determine the exact environmental loads on each structure, an estimation is sufficient in order to make a good comparison. Other loads, such as ice loading, snow loading or accidental loads due to collisions are not in the scope of this research.

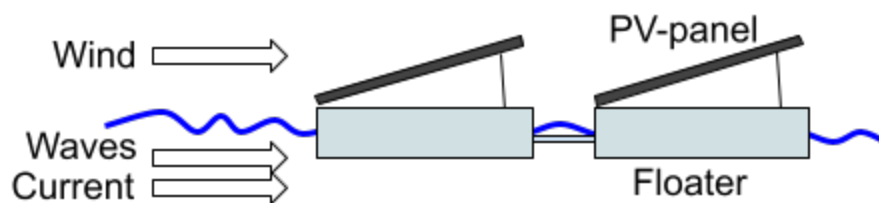


Figure 3.1: schematic drawing of loads on an FPV-structure

3.1. Wind forces

Wind forces on FPV structures are expected to be relatively high due to the usually high surface area above the water on which the wind acts. The wind force can be decomposed into the drag and the lift force. The drag force is the component of the force that is in the same direction as the wind, and the lift force is perpendicular to the wind direction. The drag and lift forces are dependent on the density of the air and the shape and size of the structure, see [Equation 3.1](#). The drag and lift coefficients (C_D & C_L) are dimensionless and dependent on the geometry of the structure and the Reynolds number. For simple shapes, such as cylinders and rectangles the coefficients can be found in literature and for complex shapes these have to be determined by experiments on (scale)models. The coefficients and the projected area depend on the direction of the wind. The drag force for a smooth cylinder, depending on the Reynolds number can be seen in [Figure 3.2](#).

$$\begin{aligned} F_D &= \frac{1}{2} * \rho * v^2 * C_D * A * C_s \\ F_L &= \frac{1}{2} * \rho * v^2 * C_L * A * C_s \end{aligned} \tag{3.1}$$

where:

ρ = Air density

v = Relative speed between wind and structure

C_D = Drag coefficient

C_s = Sheltering coefficient

C_L = Lift coefficient

A = Projected area in the direction of wind

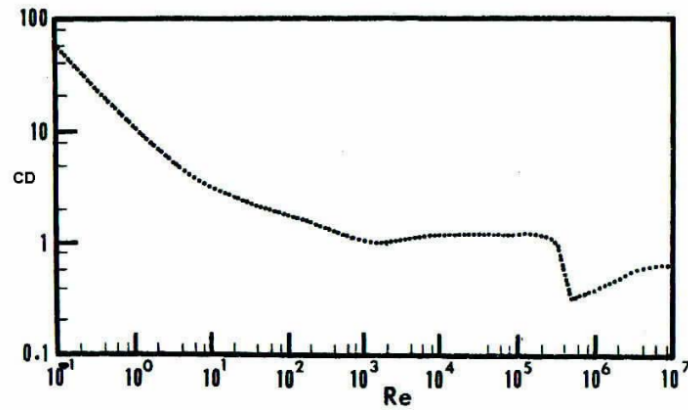


Figure 3.2: Drag coefficient for a smooth circular cylinder[25]

$$Re = \frac{V * L}{\nu} \tag{3.2}$$

where:

- V = velocity of the fluid
- L = Characteristic length
- ν = kinematic viscosity of the fluid

Sheltering

The first row that encounters the wind has a higher wind load than the second and following rows. This sheltering effect for floating PV is studied by Choi et al. [26] and a result can be seen in Figure 3.3. In their research, they found that the maximum lift and drag forces are 45%-86% lower at the centre of the structure compared to the row that first encounters the wind. Therefore a sheltering factor (C_s) is needed when calculating the wind load on multiple floaters or PV panels. This factor is highly dependent on the orientation and size of the structure.

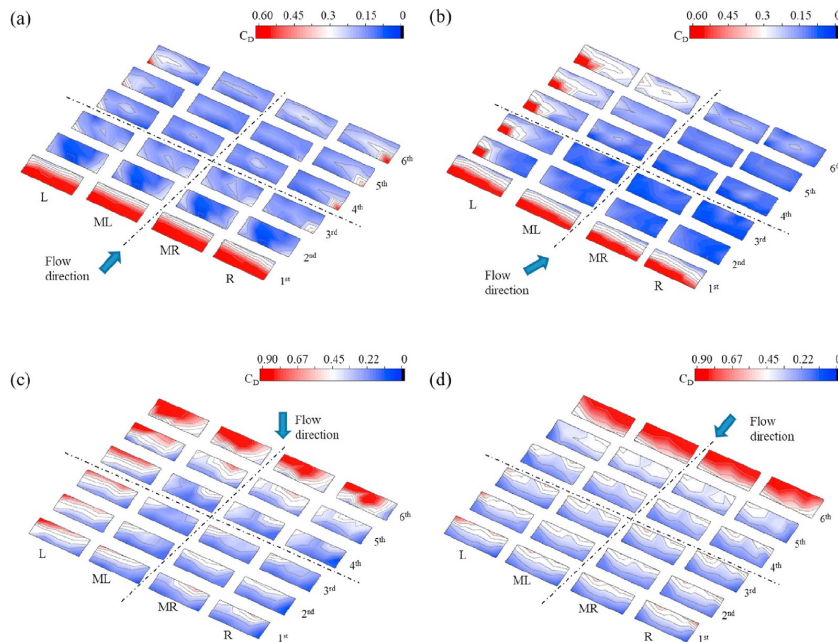


Figure 3.3: Sheltering effect on a 4 by 4 FPV structure by Choi et al. [26]

Wind angle of attack

Floating PV structures are usually placed in very open locations which means that the wind can come from all directions. It is important to design the structure for the direction that results in the highest wind loads. Choi et al. found that the lift and drag loads were the highest when the wind is in line with the structure [27]. These angles of attack of 0° and 180° are therefore the most important directions when calculating the wind loads.

Drag coefficient value PV-panels

The Drag coefficient of PV panels is highly related to the tilt angle of the panels. A PV panel can be seen as a flat plate. When the tilt angle is zero, the wind will flow over the surface and the drag force will be (close to) zero. When the tilt angle is 90 degrees, the wind will blow perpendicular to the panel and the drag force will be maximum. There are multiple studies that investigated the relation between the C_d value and the tilt angle where wind-tunnel measurements are compared to CFD simulations. The results of the studies of Mammam [28], Fadlallah [29] and Sheikh [30] are listed including the average of these studies. All values are wind angle of attack of the wind of 0 degrees, meaning the wind is acting on the front side of the panel.

Angle [deg]	0	15	30	45	90
Mammam(2018)	0.1	0.4	0.7	0.9	1.2
Fadlallah(2021)	0.1	0.3	0.5	0.7	1.5
Sheikh(2019)	0.01	0.3	0.6	0.96	1.5
Average	0.07	0.33	0.60	0.85	1.40

Table 3.1: C_d value depending on tilt angle

Wind speeds at different heights

Wind speeds are usually measured at (or corrected to) a reference height of 10m. The solar panels will be placed in a range between 0 and 3m above the water surface depending on what kind of structure is chosen. The actual wind speed at the height of each component will be lower than measured at the reference height of 10m. This wind speed can be calculated using Equation 3.3 [31].

$$U(h) = U(h_{ref}) \frac{\ln\left(\frac{h}{z_0}\right)}{\ln\left(\frac{h_{ref}}{z_0}\right)} \quad (3.3)$$

Where U is the wind speed, $z_0 = 0.002m$ is the surface roughness for water surfaces and $h_{ref} = 10m$.

3.2. Current forces

The forces resulting from the current flow can be split up into the drag and the inertia forces. The drag force is dependent on the water velocity and the inertia depends on the water acceleration. The current is assumed to be constant over a short period of time which results in the acceleration being neglectable and therefore the inertia force due to the current can be considered to be zero. The drag force due to the current is similar to the drag force due to the wind and can be seen in Equation 3.4. The symbols are the same as for the wind force except that the wind velocity is now replaced by the velocity of the current. Note that the C_D coefficient can be different for wind and water due to the dependency on the Reynolds number and fluid properties. The formula considers a load on a single body, however, when multiple bodies are present the current is influenced by the bodies upstream of the flow. Therefore a current sheltering factor should be added for the currents acting on bodies that are placed behind other bodies. For two tubes this sheltering effect can be found using Schlichting's wake formula, see Equation 3.5 [32]. For other shapes, the sheltering factor has to be found using scale-model tests of CFD simulations. The current is assumed to be a uniform horizontal flow with a constant velocity for the calculations.

$$F_D = \frac{1}{2} * \rho * u^2 * C_D * A * C_s \quad (3.4)$$

$$C_s = \left(1 - 2 * 0.95 * \sqrt{\frac{C_D * D}{CDBT + 6 * D}} \right) \quad (3.5)$$

Where:

D = Diameter of tube

CDBT = Center distance between tubes

3.3. Wave forces

Waves are irregular and calculating the loads due to waves on structures can therefore be a difficult task. In order to simplify the waves and calculations, linear wave theory can be used. In linear wave

theory, all waves are assumed to be sinusoidal. A superposition of many regular wave components, each having its own frequency, amplitude and direction, can describe an irregular sea state. In an optimal situation, long-term wave measurements are available for the location of the FPV park. These measurements can then be used to determine the maximum wave heights and find the wave loads. However, if there is no data available, an estimation of the waves can be made using the local wind speed, water depth and fetch distance.

3.3.1. Wave model

Waves caused by wind

Most waves in open water are generated by the wind. The friction between the wind and the water surface causes energy to transfer from the wind to the water and causes the water to move. For wind-generated waves, the windspeed, duration, water depth and fetch are important parameters. The fetch is the free distance from shore over which the wind has been blowing. Wind waves can be limited by the duration of the wind or the maximum fetch. A distinction can be made for determining the wave spectrum for deep or shallow-water waves and both are explained below.

Deep water conditions

Assuming deep water conditions the significant wave height can be determined with the fetch and the windspeed using the relation from Figure 3.4 [33]. Where all variables with a tilde (\sim) on top are made dimensionless. It is important to note that in this equation the significant wave height (H_s) is calculated and not the maximum wave height. Assuming the waves follow a Rayleigh distribution, waves up to twice the significant wave height should be expected to occur [34]. When the significant wave height is calculated with the maximum fetch and the highest daily average wind speed that is expected in 50 years, the estimated value can be assumed to be the maximum expected wave height in 50 years for waves generated by the wind.

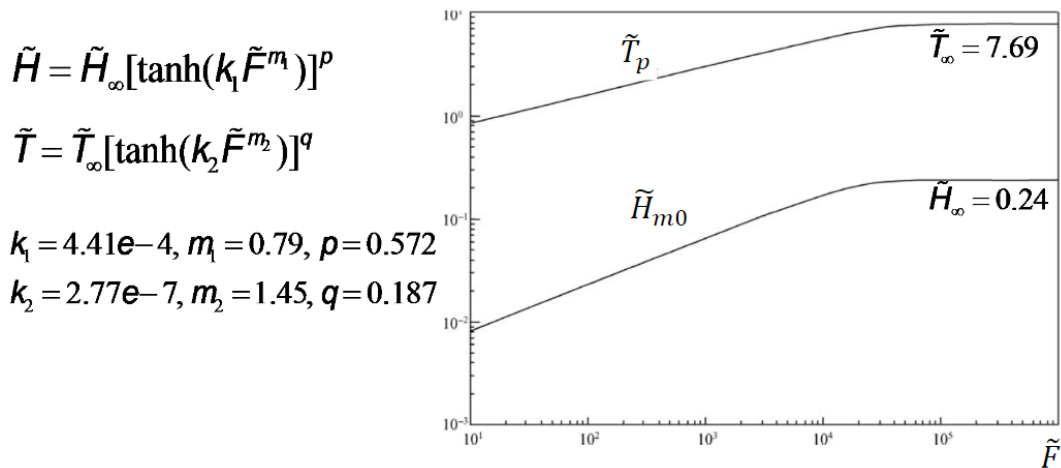


Figure 3.4: Dimensionless relation wave height and fetch [33]

$$\tilde{F} = \frac{g * F}{U_{10}^2}$$

$$\tilde{H} = 0.24 * [\tanh(4.41e^{-4} * \tilde{F}^{0.79})]^{0.572} \quad (3.6)$$

$$H_s = \frac{U_{10}^2 * \tilde{H}}{g}$$

$$H_{max} \approx 2 * H_s$$

$$\tilde{T} = 7.69 * [\tanh(2.77e^{-7} * \tilde{F}^{1.45})]^{0.187}$$

$$T_p = \frac{U_{10} * \tilde{T}}{g} \quad (3.7)$$

For the above formulas to be valid the location must be categorised as deep water conditions. For deep water conditions to be valid the water depth must be larger than half the wavelength. The wavelength can be found using the dispersion relationship, see Equation 3.8.

$$L = \frac{g * T^2}{2\pi} * \tanh\left(\frac{2\pi * d}{L}\right) \quad (3.8)$$

where:

L = Wavelength

T = Wave period

d = Water depth

Shallow water spectrum

A wave spectrum describes how the energy of waves is distributed over different frequencies. There are multiple models created for different conditions and locations. The input for these models are the wind velocity, wave characteristics and measurements in the field of historical data. Examples of wave-spectra models for deep waters are the Pierson-Moskowitz or Jonswap (Joint North Sea Wave Project) models. However, for the location at Haringvliet a model is needed that takes the limited water depth into account. For shallow water, a TMA (Texel-Marsen-Arsole) spectrum can be used. In this spectrum a factor is added so the influence of the finite water depth is included. The factor ϕ depends on the frequency and the water depth. The model of Bouws et al. (1985) [35] added the extra factor to the Jonswap spectrum, and this spectrum is given in Equation 3.9.

$$E(f) = \frac{\alpha * g^2}{(2\pi)^4 * f^5} \exp\left[-\frac{5}{4}\left(\frac{f}{f_p}\right)^{-4}\right] * \gamma^{\exp\left[\frac{-(f-f_p)^2}{2 * \sigma^2 * f_p^2}\right]} * \phi(2\pi f, h) \quad (3.9)$$

where:

$$\alpha = 0.0078 \left[\frac{2\pi * V_{10}^2}{g * L_p} \right]^{0.49}$$

$$\gamma = 2.47 \left[\frac{2\pi * V_{10}^2}{g * L_p} \right]^{0.39}$$

$$\phi(2\pi f, h) = \omega_h^2 / 2 \text{ for } \omega_h \leq 1$$

$$\phi(2\pi f, h) = 1 - 0.5 * (2 - \omega_h)^2 \text{ for } \omega_h > 1$$

$$\sigma = 0.07 \text{ for } f \leq f_p$$

$$\sigma = 0.09 \text{ for } f > f_p$$

$$f_p = \frac{3.5 * g}{V_{10}} \left[\frac{g * F}{V_{10}^2} \right]^{-0.33} = \text{Peak frequency}$$

$$L_p = \text{Wavelength corresponding to } f_p$$

Waves caused by ships

Next to the wind waves, waves can also be caused by ships that are passing by. These ships can be split up into two categories. The first one is commercial ships such as freight ships and dredging ships. The second one is for pleasure and contains mainly smaller sail- and speedboats. The commercial ships are often very large with a high draft and will create larger waves with more energy while the smaller ships will create waves with higher frequencies. Due to the lack of data on these ships and lack of time to further investigate the responses, the waves caused by ships are not taken into account in this thesis.

3.3.2. Morison equations

The wave load on slender structures can be calculated by the Morison equations. Morison et al. [36] showed that the force on a tubular pile per unit of length can be found by adding a drag and an inertia component, see Equation 3.10. The drag component depends on the velocity of the fluid (u) and the inertia component on the acceleration (\dot{u}). All symbols are similar to the drag equation for the current, except the inertia force (F_i) and inertia coefficient ($C_m = 1 + C_a$). Where C_a is the added mass coefficient. Note that in this equation V is the volume of the object and not a velocity and L is the characteristic length of the object. There are some limitations on the use of the Morison equations. One is that the characteristic length of the object of the cylinder should be much smaller than the wavelength. The equation is designed to long vertical cylinders and therefore often used in Offshore applications such as jacket structures. These equations can therefore be used when analysing the wave loads on FPV structures with elevated decks such as the Seavolt or Solarduck designs. For other structures that use floaters near the waterline, the equation can give less accurate results [37].

$$F = F_d + F_i = \frac{1}{2} * \rho * C_D * L * u * |u| + \rho * C_M * V * \dot{u} \quad (3.10)$$

In order to compute the wave-forces the velocity and acceleration of the water-particles are needed. If there is wave data available this can be used to obtain the velocities accelerations and forces. If there is no long-term wave data available, a wave elevation profile can be created from the wave spectrum. From this wave elevation, the velocity and the acceleration of the water particles can be computed.

4

Calculations on existing structures.

In this chapter, the loads acting on different structures will be calculated. First, the assumptions and simplifications made for the calculations are presented. Then an overview of the steps taken to find the environmental loads is given and these steps are explained in detail. All these steps are performed for three different structures, for the first structure (*Floating Solar*) the steps taken and equations used are fully explained. For the other systems the same steps are taken and only the differences and results are shown. In [section 4.7](#), the results of all systems are compared and visualised.

4.1. Assumptions for calculations

Finding the exact forces due to the environmental loads is a challenging and complex task. In order to find these loads within the scope and time of this research some simplifications and assumptions are needed. An overview of these assumptions is given below together with an explanation and the consequences.

Assumption 1 *Maximum expected load*

This research aims to find the maximum expected load for three different types of FPV structures. This means that for the wind, waves and current the maximum expected values, with a return period of 50 years, are used. Furthermore, only the forces in the horizontal direction are calculated in this thesis.

Assumption 2 *Simplifications in models*

To find the load on each structure, a simplified model is made to represent a part of the structure. For these models, only the most important components are taken into account. These components such as the solar panels and floaters, are then replaced by standard shapes. The loads on other components are neglected. Examples of these components are the connection pieces, boat access areas, transformers and combiner boxes. Analysing the loads on all these components is not needed in order to compare the different systems and would require too much time within the scope of this research.

Assumption 3 *Angle of attack*

The angle of attack for all loads is taken as 0° , which means that the loads act perpendicular to the structure. For this situation, the frontal area of the floaters and panels is the largest and therefore the loads are assumed to be the highest. More research can be done to analyse the effects of different angles of attack.

Assumption 4 *Uniform constant current velocity*

The current velocity is assumed to be constant and uniform, which implies that the current has no acceleration. In reality, the current would be variable over time and over the water depth. Taking the maximum current at each point would overestimate the loads while neglecting the acceleration component underestimates the current load.

Assumption 5 *Waves are unidirectional*

The assumption is made that the waves are unidirectional, which means that the waves are propagating in only 1 direction. For the calculations, the waves propagate in the x-direction perpendicular to the system and are therefore constant over the y-direction.

Assumption 6 *Combination waves and current*

For the combination of the waves and current the velocity of the current is added to the x-component of the velocity for the waves. With this method, the direction of the waves and current is aligned increasing the total water velocity. To find the wave forces, this velocity is squared and therefore the waves and current cannot be found independently and later be added. Having a current in the opposite direction of the waves can increase the steepness of the waves and therefore also increase in impact the waves have on the structure. However, analysing the effects of different current and wave directions is not in the scope of this research.

Assumption 7 *Wind sheltering*

The sheltering effect of the wind is a complex phenomenon that depends on the structure's geometry, the wind velocity and the turbulent intensity of the wind. In order to make the calculations simpler, a constant sheltering factor of 40% is used for the second row of the structures and 15% for rows three and further. These factors are found using data from an FPV park that is operated by *Floating Solar*.

Assumption 8 *Wave structure interaction*

The assumption is made that the structures do not have an influence on the waves. In reality, the structure would have a damping effect on the waves limiting the amount of energy that is transmitted. This would lower the wave forces on parts of the structure that are in the wake of other parts. On the other hand, the interaction between the waves and structure can also increase the loads. This happens when the frequency of the waves is close to the eigenfrequency of the structure. The structure will start to resonate, increasing the amplitude of the motions. This can lead to high internal forces and even cause failures. To prevent this the structure should be designed in a way that the eigenfrequency is not close to peaks in the wave spectrum. The effects of wave structure interaction can be analysed in further research.

Assumption 9 *Constant water depth*

The water depth is assumed to be constant over the entire area of the project. In reality, the water depth decreases near the shoreline and this causes the waves to break. Breaking waves can have a high impact on the structures. Due to the assumption of constant water depth, the effects of wave breaking is not taken into account in this research.

Assumption 10 *Friction coefficient wind*

The friction coefficient of air on the membrane with PV panels was unknown and not found in the literature. Therefore the assumption is made that the glass of the PV panels would have a friction coefficient that is close to the friction coefficient of an ice floe, due to the similarities in the surface roughness.

4.2. *Input parameters*

The maximum expected loads for the lifetime of the structures are calculated. This means that the wind, wave and current loads are calculated with the maximum expected values for a 50-year return period. The loads can be applied in any direction on the structure, however, for the ULS the focus is only on the direction that results in the highest loads, where the angle of attack is 0 degrees. The loads are all calculated with the site conditions found for the case study location Haringvliet. See [chapter 6](#) for the detailed description of how these conditions are found and [Table 4.1](#) for an overview of input parameters.

Wind		Symbol	Value	Unit
	Maximum wind-gust at 10m	$V_{10,gust}$	41.2	m/s
	Maximum daily average at 10m	$V_{10,daily}$	18.6	m/s
	Dominant direction		South-West	
Current				
	Maximum current	C	0.67	m/s
Waves				
	Significant wave height	H_s	0.75	m
	Maximum wave height	H_{max}	1.50	m
Other				
	Fetch	F	3	km
	Water depth	d	5	m
	Density water	ρ_w	1000	kg/m ³
	Density air	ρ_A	1.25	kg/m ³

Table 4.1: Environmental input parameters of location

4.3. Method for calculations

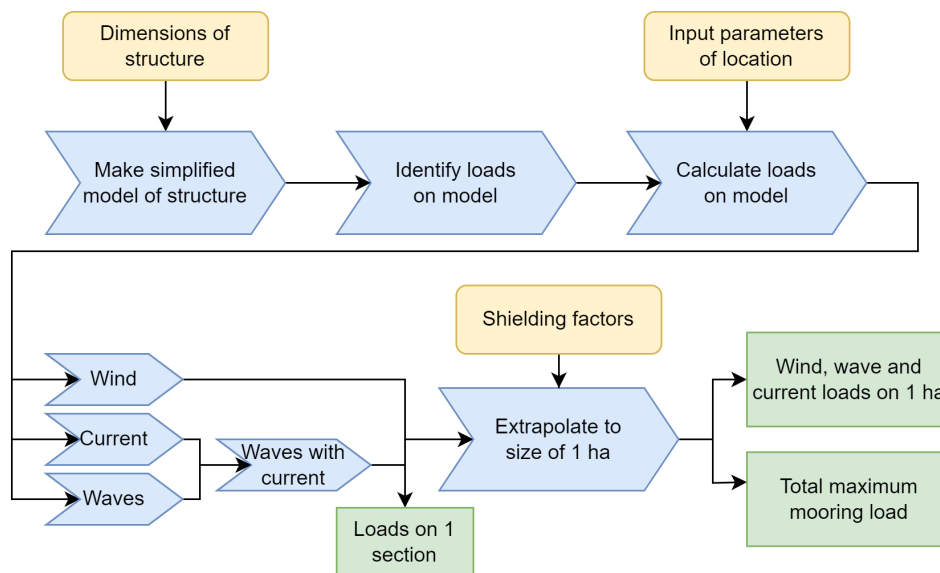


Figure 4.1: Flowchart for calculations

1. Dimensions

The first step is to understand the principal concept of the FPV structure and collect all the necessary dimensions of the structure. This includes the dimensions of the floater, the panels, the frame and also the distances between the panels or floaters, number of panels per floater and the size of a standard island.

2. Simplified model

Often an FPV structure is built up of a relatively simple concept that is then repeated to create a large floating structure. The second step is to identify the floaters and make a simplified model of a small element of the structure, see [Figure 4.2](#) for an example. Finding the load on this small part is easier than trying to find the loads on the entire structure. Once these loads are found an extrapolation can be made to find an estimation of the total loads.

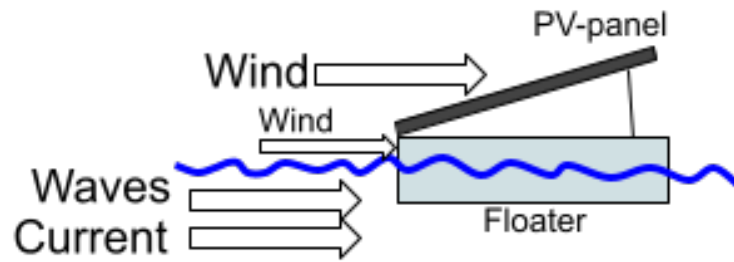


Figure 4.2: Simplified example model with environmental loads

3. Identify environmental loads

When a simplified model is created, the environmental loads that act on the structure can be identified. Above water it is only the wind load, this can act on the panels, the part of the floaters above water and on the frame. The wind can also act as a friction force if the system has a very large flat surface. Underwater the current and waves will act on the part of the floaters that is submerged.

4. Calculate loads on model

Now the loads can be calculated on one single element for 1 section per meter length. The results of this step give the loads by the wind, waves and current on one row or section per meter length.

(a) Wind

Convert the maximum wind gust to the height above mean sea level of each element. Find C_d values for the different elements that experience a drag force due to the wind. The C_d values depend on the Reynolds number and the geometry of the element. Now use the equation in [section 3.1](#) to find the drag force on each element. The total drag force due to the wind on 1 section per meter length can then be found by adding up the individual drag forces. In the example, this will be the wind acting on the panel and the wind acting on (a part of) the floater.

For very large surfaces, the friction forces due to the wind can be significant. In that case, find the flat area on which the wind friction can act and find the friction coefficient between the surface and the wind. Note that this force is directly calculated for a larger area and not for a section per meter length.

(b) Current

The current will only result in a load acting on the part of the floater that is underwater. A new C_d value is needed for the floater because water is now the medium instead of air which can result in different Reynolds numbers and thereby C_d values. Use the equation from [section 3.2](#) to find the drag force due to the current.

Again, for large surfaces, such as membrane structures, there can also be a significant friction force.

(c) Waves

In order to find the wave forces it is necessary to know the wave conditions. In the best scenario, long-term measurements are available of which the significant and maximum expected wave heights can be found. If this is not available a time-series can be created from a wave spectrum. The wave spectrum can be found with the wind speed, fetch length and water depth. If the elevation over time and thereby the velocity and acceleration of the water particles is known, [Equation 3.10](#) can be used to find the drag and inertia forces. The wave force is then found by adding the inertia and drag forces, see [Equation 4.1](#).

$$F_{total} = F_d + F_i \quad (4.1)$$

(d) Waves + current

The wave and current loads can not just be added up to find the total forces. This is because the total forces are dependent on the velocity squared, and adding the forces up later will result in an error for the total force. Therefore the velocity of the current (u_0) has to be added to the velocity of the water due to the waves (u). Note that the velocity of the current

is a constant factor and is added only to the x-component of the velocity. The rest of the calculation is similar as for only the waves. With this approach, the waves and current will both come from the same direction see assumption 6.

5. Extrapolate to 1 ha

Because all systems can have very different sizes and shapes, it is difficult to compare the loads on a single section. Therefore an extrapolation of the forces is made to find the total force on a larger area. A standard area of 1 hectare (100m by 100m) is chosen, this is for most systems as a rule of thumb equal to a FPV park with a capacity of 1 MWp. As an input for the extrapolation, a shielding factor for the wind and current is needed. This shielding factor is dependent on the geometry of the FPV park, it deals with the phenomenon that the first (and second) row will block a part of the wind and current for the rows behind. To find the wave forces for the total structure, the forces are simultaneously found for each floater and added up. With this method, the wave force for the entire structure can be found that is a function of time. It takes into account that the largest wave does not hit every row of floaters at the same time. Finding the wave forces on one floater and multiplying it by the number of floaters would give inaccurate and very high results.

The result of these calculations is an individual wind, current and wave force and a force for the current included in the waves per structure. The total maximum load can then be found by adding the wind force to the force of the waves including the current. The maximum load is the load that the mooring system of the structure should be able to withstand.

4.4. Floating Solar (Company)

The base of the design of the structure from *Floating Solar* consists of large high-density polyethylene (HDPE) tubes for buoyancy. On the tubes, a metal frame is placed on which the solar panels are mounted with a tilt angle of 30 degrees. Multiple rows are connected by the metal frame and form a circular island. The island is able to rotate around the vertical centre axis of the island to let the panels face the sun directly and increase the energy yield. Figure 4.3 is a picture of the design from *Floating Solar* and in Figure 4.4 a schematic image showing a simplified model used for the calculations. In this image, the forces acting on the structure are shown. Above the waterline, only the wind acts on the structure. Underwater the forces are due to the current and waves and only act on the part of the tube that is submerged. All dimensions can be found in Appendix A, the most important steps for the calculations are explained below.



Figure 4.3: Floating Solar design [21]

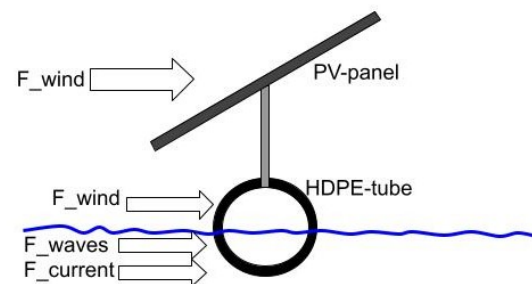


Figure 4.4: Schematic image of Floating Solar design

4.4.1. Wind force

The wind load is first calculated for a section of 1 row with a length of 1 meter. The wind load is split up into two parts, namely the part acting on the panels and the part acting on the tubes. The first step is to analyse the wind force on the tube. The tube is semi-submerged and the wind will only act on the part above the waterline. As mentioned in section 3.1 the windspeed is highly dependent on the height, it is necessary to find the windspeed at the height of the tube using Equation 3.3. The maximum wind gust for 50 years at a height of 10 cm is $18.92 \frac{m}{s}$. At this windspeed, the Reynolds-number for the tube is approximately $Re = 4 * 10^5$, which results in a drag coefficient of 1.0, see Figure 3.2. The factor $(1 - \alpha)$ is used to scale the force with the area of the tube that is above the water. Where α is the

relative draft of the tubes that are found with the total weight of the structure and the buoyancy of the tubes.

$$F_{D,tube} = \frac{1}{2} * \rho * v^2 * C_{D,tube} * (1 - \alpha) * D = 37.85 \frac{N}{m} \quad (4.2)$$

where:

$$\rho = \text{Air density} = 1.25 \frac{kg}{m^3}$$

$$v = \text{Maximum wind-gust at 10 cm} = 18.92 \frac{m}{s}$$

$$C_{D,tube} = \text{Drag coefficient tube} = 1.0$$

$$1 - \alpha = \text{part of tube above water} = 0.54$$

$$D = \text{Diameter of the tube} = 0.315 \text{ m}$$

The second part of the wind force acts on the PV panel and the equation for the drag force has to be adjusted to the shape of the panel. The panel is mounted on a frame with an average height of 1m and that is the height used for the windspeed. The panels are mounted in landscape orientation under a tilt angle of 30 degrees, which influences the frontal area of the panel. The Cd value for the panel with this tilt angle can be found in [Table 3.1](#).

$$F_{D,panel} = \frac{1}{2} * \rho * v^2 * C_{D,panel} * \sin \theta * P_W = 369 \frac{N}{m} \quad (4.3)$$

where:

$$v = \text{Maximum wind-gust at 1m} = 30.06 \frac{m}{s}$$

$$C_{D,panel} = \text{Drag coefficient panel} = 0.6$$

$$\theta = \text{Tilt angle} = 30^\circ$$

$$P_W = \text{Width of panel} = 1.134 \text{ m}$$

$$F_{D,total} = F_{D,tube} + F_{D,panel} = 192 \frac{N}{m} \quad (4.4)$$

Now the wind load on a single section per meter length is known, the next step is to extrapolate the wind loads to the larger standard area of 1 hectare with multiple rows. The spacing between two rows is 1.8 m, resulting in 55 rows in 100 m. The first row will encounter the wind load as found in [Equation 4.4](#), the rest of the rows will have a much lower wind loading due to the sheltering effect as shown in [Figure 3.3](#). H. Engberts from the company *Floating Solar* shared during a meeting that the sheltering effect they found is between 80% and 90% for the middle rows and 40% for the second row. These values are found by a CFD-analyses of the structure in combination with measurements in the field [38]. The second row has a sheltering factor of $S_{row2} = 0.40$ and the rows in the middle (row >2) of the structure will only receive 15% ($S=0.15$) of the wind load. Using this sheltering factor, a length of 100m and 55 rows, the total drag force due to the maximum wind-gust in 50 years will be 371kN, see [Equation 4.5](#).

$$\text{Windload} = F_{D,total} * 100 * (1 + S_{row2} + S * (\text{Rows} - 2)) = 215 \text{ kN} \quad (4.5)$$

4.4.2. Current force

The current will only result in a load acting on the part of the tube that is underwater. The drag force due to the current is very similar to the drag force due to the wind. The new Reynolds number for the tube in water is $Re=2.0E5$, resulting in a drag coefficient of again 1.0, see [Figure 3.2](#). The draft of the tube is 46% of the diameter, the factor α is added to the equation.

$$F_{D,current} = \frac{1}{2} * \rho * C_d * \alpha * D * u^2 = 30.8 \frac{N}{m} \quad (4.6)$$

Where:

$$\rho = \text{Density of water} = 1000 \frac{kg}{m^3}$$

$$u = \text{max velocity of current} = 0.65 \frac{m}{s}$$

$$C_d = \text{Drag coefficient tube water} = 1.0$$

$$\alpha = \text{Draft/diameter} = 0.46$$

The current also experiences a sheltering effect, which can be calculated by Schlichting's wake formula, presented in Equation 3.5 and filled in for the *Floating Solar* tubes in Equation 4.7.

$$SH_c = 1 - 2 * 0.95 * \sqrt{\frac{C_d * D}{\Delta X + 6D}} = 0.445 \quad (4.7)$$

Where:

D = Diameter tube = 0.315m

ΔX = Spacing between two tubes = 1.8m

Now the total drag force due to the current for 1 hectare can be calculated using Equation 4.8.

$$Currentload = F_{D,current} * 100 * (1 + SH_c * (Rows - 1)) = 77.1kN \quad (4.8)$$

4.4.3. Wave force

The wave-load can be computed using the Morison equation presented in Equation 3.10. The equation has to be adjusted to match the semi-submerged cylinder. The length and volume now depend on the diameter of the tube and the same factor α is added in order to neglect the part that is above the waterline.

$$F = F_d + F_i = \frac{1}{2} * \rho * C_D * \alpha * D * u * |u| + \rho * C_M * \alpha * (\pi * (\frac{D}{2})^2) * \dot{u} \quad (4.9)$$

Where:

$C_D = 1.0$ (Re= $5 * 10^4$)

$C_M = 1 + C_A = 2.0$ [39]

α = Draft/Diameter = 0.46

Using Equation 4.9 and the velocity(u) and acceleration(\dot{u}) from the wave spectrum, see Figure B.3 and B.4, the drag and inertia forces can be found. The total force can be calculated by adding the drag and inertia forces. The forces on one section can be seen in Figure 4.5. Note that only a small section of the time series is shown in the plots. The maximum wave load on the tube can be found where the wave force is the highest. The highest wave force per meter for the tube is $469 \frac{N}{m}$.

In order to find the wave force for the entire structure, the forces on each row are found simultaneously and added. The total wave force on the structure is a function over time and can be seen in Figure 4.6. No sheltering factor is used for the extrapolation of the wave force to an area of 1 hectare. This is due to the assumption that the structure has no significant influence on the waves, see assumption 8. The total maximum wave load for 1 hectare is 163 kN.

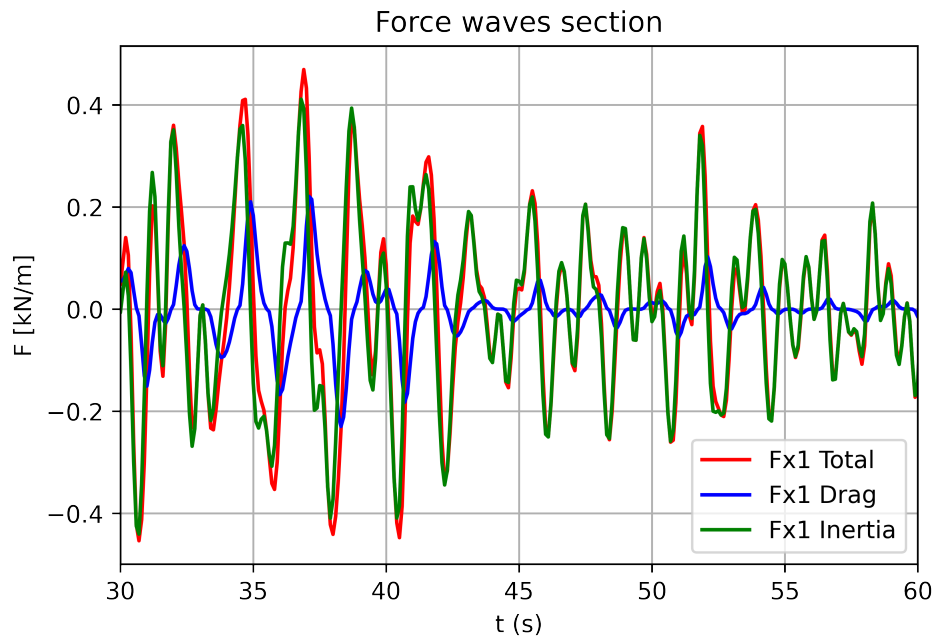


Figure 4.5: Drag, inertia and total force on one section

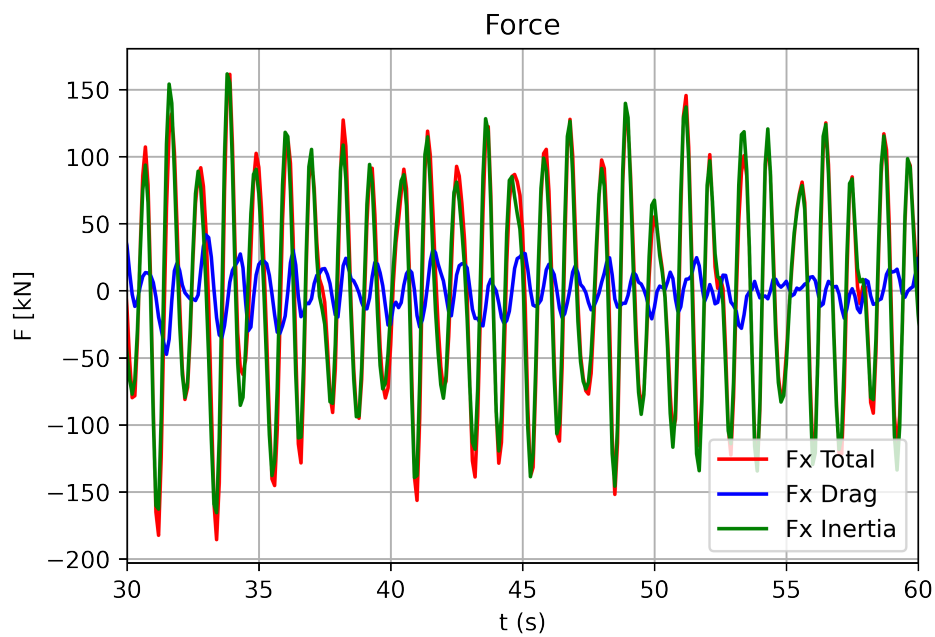


Figure 4.6: Wave forces entire structure

4.4.4. Waves + current

The method is similar for only the waves with the only difference that the current velocity is added to the x-component of the velocity of the waves, see assumption 6. This results in a maximum force of 606N per meter tube, and a total maximum force of 462 kN for 1 hectare.

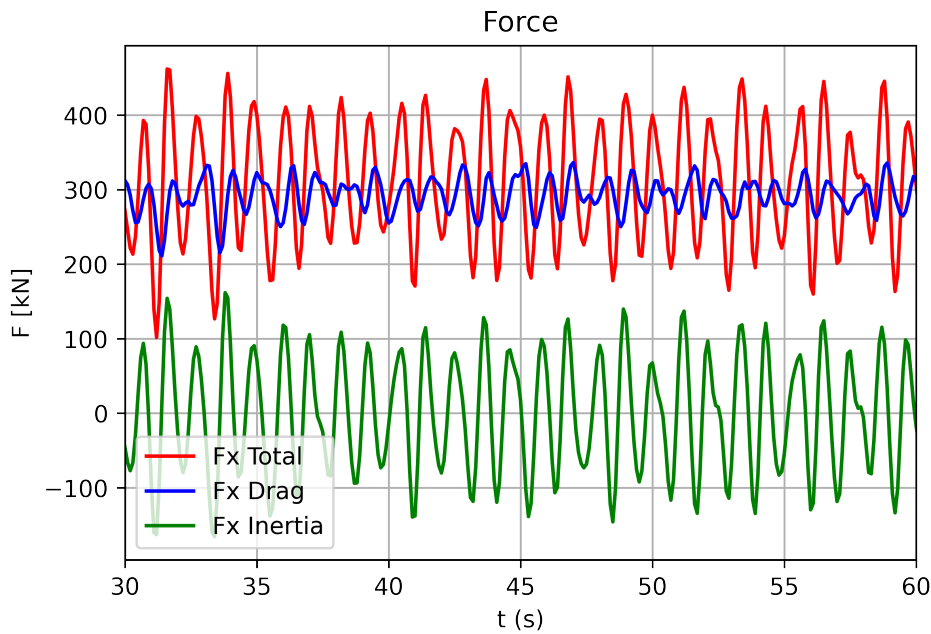


Figure 4.7: Wave forces entire structure with current

4.4.5. Overview of the forces

In the table below is an overview of the wind, current and wave forces found for the *Floating Solar* structure. The order of magnitude is presented in this table in order to account for the inaccuracy due to some simplifications and assumptions made in the calculations. From the table, it can be seen that the waves result in the highest loads, followed by the wind and that the current has the lowest impact on the structure.

	1 section [N/m]	1 ha, (100x100m) [kN]	Order of magnitude [N]
Wind	230	215	10^5
Current	30.8	77.1	10^5
Waves	469	163	10^5
Waves + current	606	462	10^6
Total mooring load	836	677	10^6

Table 4.2: Overview of forces on *Floating Solar* structure

4.5. Ocean Sun, flexible membrane

The design of the FPV structure from the Norwegian company Ocean Sun is a flexible membrane with circular buoyancy rings. The membrane allows the structure to move along with the waves, resulting in lower wave forces. These buoyancy rings have their roots from offshore fish farms where they are used to keep the fishnets in place. Between the buoyancy ring a very thin (1 mm) and flexible membrane is placed. This reinforced membrane is made of a similar material as used to cover trucks. Standard PV panels are placed on the membrane using a double keder connection. Around the structure there is a small vertical railing, 80 cm above the buoyancy rings for safety. Bilge pumps are placed on the membrane to remove (rain)water. The islands are available in multiple sizes and can be adjusted for each location. Standard sizes for the islands are 50, 66 or 72 meters in diameter. For the calculations the island with a diameter of 72m is chosen that has a capacity of 670kWp. The total weight is 55 tons including all panels, pumps, rings and the membrane [40]. The buoyancy tubes are placed almost directly next to each other and are connected with brackets, therefore they will act to the forces as one structure. The area of an island is 4071 m^2 , for comparison the total forces are divided by this area and multiplied by the standard area of 1 hectare.



Figure 4.8: Ocean Sun, flexible membrane

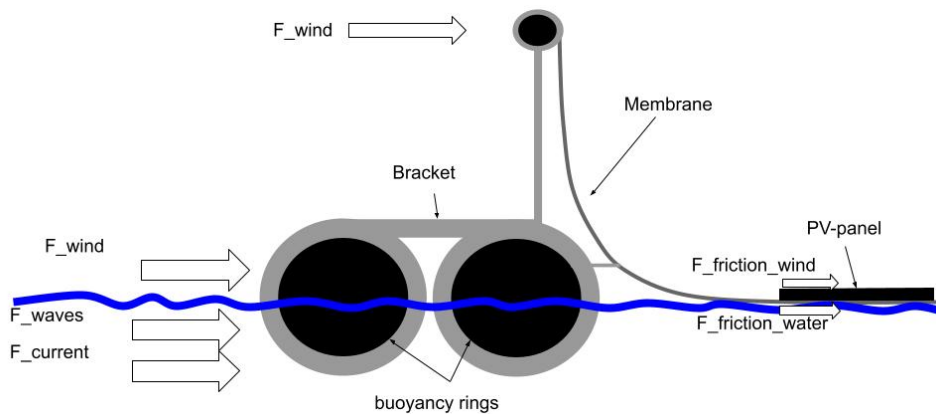


Figure 4.9: Schematic image of Ocean Sun design

4.5.1. Wind force

The structure is designed to be as close to the surface as possible in order to minimise the wind forces. The drag force of the wind can only act directly on the part of the buoyancy rings that is above water and on the safety railing. Next to these direct loads, the wind will also act on the membrane as a frictional force because the surface is perpendicular to the wind. The wind load on the tubes is very similar to the *Floating Solar* structure and can be computed with the same method. All dimensions and coefficients can be found in [Table A.3](#) in [Appendix A](#). The wind velocity is adjusted to the height of the tubes and the railing. The load is first found per meter for the tubes and for the railing. Then the load per meter is integrated over the circumference of the island in order to find the total wind load on the tubes, see [Equation 4.10](#) where r is the radius of the island. The wind load on the tubes per meter and for the island can be found in [Table 4.4](#).

$$\int_0^{2\pi} F/m * \cos(\theta)^2 * r d\theta \quad (4.10)$$

Friction force

The wind also acts on the membrane as a friction force. The friction force can be found using [Equation 4.11](#). Here the friction coefficient ($C_{F,air} = 0.002$) is the friction coefficient between an ice floe and the wind [41]. This is chosen due to the lack of data on the exact friction coefficient between the panels and the wind. The assumption here is that glass and ice will have a relatively equal friction coefficient, see assumption 10. The wind velocity is set at a height of 5cm above the surface of the membrane, this is approximately the thickness of the panels including the mounting keders.

$$F_{fric,A} = A * C_{F,air} * \frac{1}{2} * \rho_{air} * V^2 \quad (4.11)$$

Where:

$A = \text{area of the membrane} = 4071m^2$

$C_{F,air}$ = Friction coefficient = 0.002

ρ_{Air} = density air = $1.25 \frac{kg}{m^3}$

V = wind velocity at 5cm = $15.6 \frac{m}{s}$

4.5.2. Current force

The current force on the structure will act on the part of the buoyancy tubes that is underwater and as a friction force on the membrane. The force on the tubes is found in the same way as for the wind on the tubes, namely first per meter of the tube and then integrated over the circumference of the island. Note that there are two tubes next to each other and the second tube will have a much lower force due to the sheltering effect. This Sheltering factor for the tubes is 0.1, meaning that the second tube only receives 10% of the load that the first tube has. The current load per meter of tubes is 36.4N and for the island 4.12 kN.

The friction of the current on the membrane can be found using Equation 4.12. Now the friction coefficient is for the friction between the water and the membrane given by Are J. Berstad and Petter Grøn [42]. The friction load of the current is 2.75 kN for the island, see Table 4.4.

$$F_{fric,c} = A * C_{F,c} * \frac{1}{2} * \rho_W * C^2 \quad (4.12)$$

Where:

A = area of the membrane = $4071m^2$

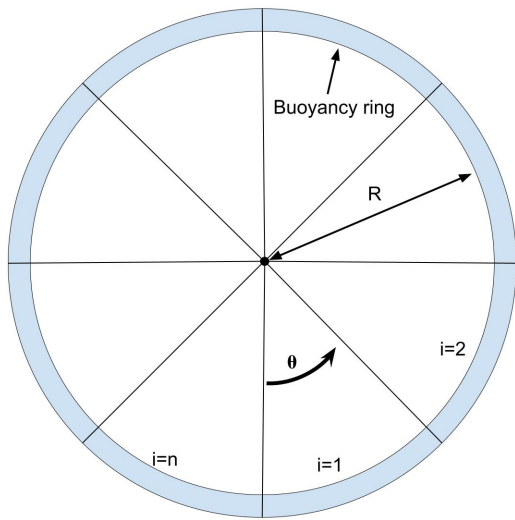
$C_{F,c}$ = Friction coefficient = 0.0032

ρ_W = density water = $1000 \frac{kg}{m^3}$

C = Current velocity = $0.65 \frac{m}{s}$

4.5.3. Wave force

For calculating the wave forces on the tubes the same procedure is used as for the *Floating Solar* structure, given in subsection 4.4.3. Using the velocity and acceleration retrieved from the TMA-spectrum, the Morison equation given in Equation 4.9 can be computed. The maximum wave load on a section of the tubes is $600 \frac{N}{m}$. Due to the large area of the entire structure, this force can not be scaled up using Equation 4.10. The wave forces on the buoyancy rings will vary over the circumference, therefore the forces need to be found for a small element of the ring and then integrated over the angle of that element. The first step is to divide the buoyancy rings into n number of elements, see Figure 4.10. Then for each element, the angle θ and corresponding x-coordinate are found. At this x-coordinate, the wave forces as a function of time are computed and then added for each integration element to get the total wave force on the buoyancy rings. For the final calculation, 400 elements were used to find the total force, increasing the number of elements higher than 200 elements did not alter the final outcome. In Figure 4.11 and 4.12 the graphs of the wave forces on the buoyancy tubes are given. Here it can be seen that the current increases the total for each time step and shifts the graph up. This is because the current is a constant velocity in the positive x-direction and therefore increases the total force on the tubes in the x-direction.



$$\begin{aligned} \theta_i &= (i/(n-1)) * 2 * \pi \\ x_i &= R - R * \cos(\theta_i) \end{aligned} \quad (4.13)$$

$$F_{tot} = \sum_{i=1}^{i=n} \int_{\theta_i}^{\theta_{i+1}} F(x_i) * \cos(\theta)^2 * R d\theta$$

Figure 4.10: Integration steps waves on buoyancy ring

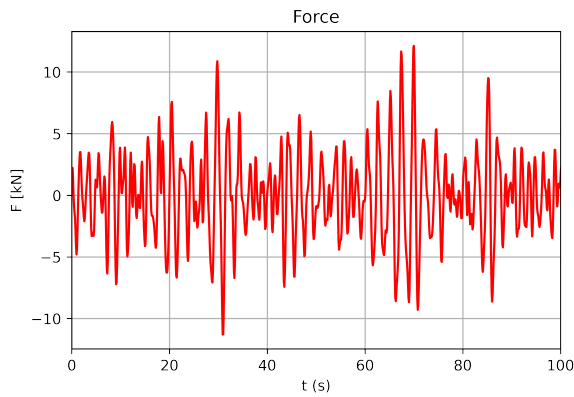


Figure 4.11: Wave force on tubes only waves

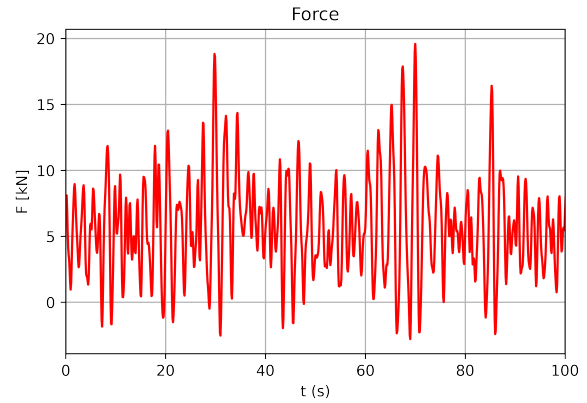


Figure 4.12: Wave force on tubes waves with current

Friction forces of the waves

The friction forces of the waves have the same principal formula as for the current. The difference is that the current was assumed to be constant over time and the membrane, which is not the case for the waves. The velocity of the waves at the water surface ($z=0$) can be found using Equation 4.14. Here the velocity depends on the time and the x -coordinate. Therefore the friction force has to be found at multiple points on the membrane and then integrated over the corresponding area. The final friction force for the island will remain a function of time. The waves are assumed to be constant over the y -direction (see assumption 5), therefore the membrane is only divided in the x -direction as can be seen in Figure 4.13. For each point of x_i the velocity of the waves is calculated from the given spectrum. This velocity (still a function of time) is then used in Equation 4.16 to find the friction force per area and the total friction force of the island. In the figure, the x -coordinate is divided into 10 steps of x_i to visualise the method, for more accurate results the calculation is performed with many more steps. In Figure 4.14 the friction force of only the waves and the waves including the current can be seen as a function of the number of steps. The plot shows that the friction forces converges to a stable value after 200 points. Increasing the number of iteration points even further does not change the outcome.

$$v_w = a * \omega * \tanh(k * h) * \sin(k * x - \omega * t + \phi) \quad (4.14)$$

a = Amplitude of the wave
 ω = wave frequency

$k(= \frac{2\pi}{\lambda})$ = Wave number
 h = Water depth
 x = Coordinate in surge direction
 ϕ = Phase

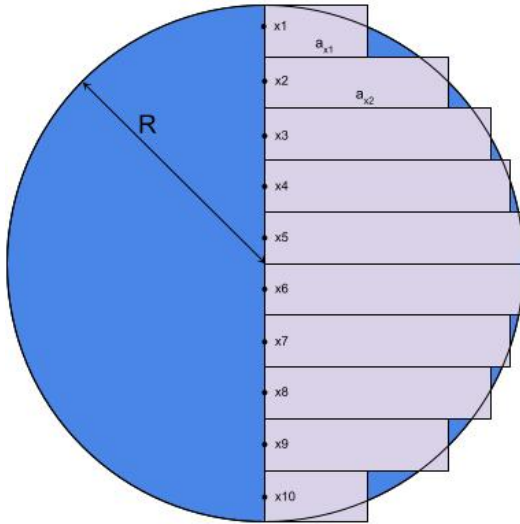


Figure 4.13: Integration steps Ocean Sun

$$\begin{aligned} \text{(For } x_i < R) \quad a_i &= \sqrt{R^2 - (R - x_i)^2} \\ \text{(For } x_i \geq R) \quad a_i &= \sqrt{R^2 - (x_i - R)^2} \end{aligned} \quad (4.15)$$

$$\text{Area}_i = 2 * a_i * (x_2 - X_1)$$

$$F_i(t) = \frac{1}{2} * \rho_W * C_{F,c} * v_x(t) * |v_x(t)| * \text{Area}_i$$

$$F_{\text{island}}(t) = \sum_{i=1}^{i=n} F_i \quad (4.16)$$

Number of steps	Waves [kN]	Waves with current [kN]
2	17.6	32.3
10	5.06	14.3
20	1.90	7.83
40	1.012	6.94
100	0.556	6.329
200	0.376	6.056
400	0.364	6.055
600	0.364	6.054

Table 4.3: Friction force of waves and waves with current vs. number of integration steps

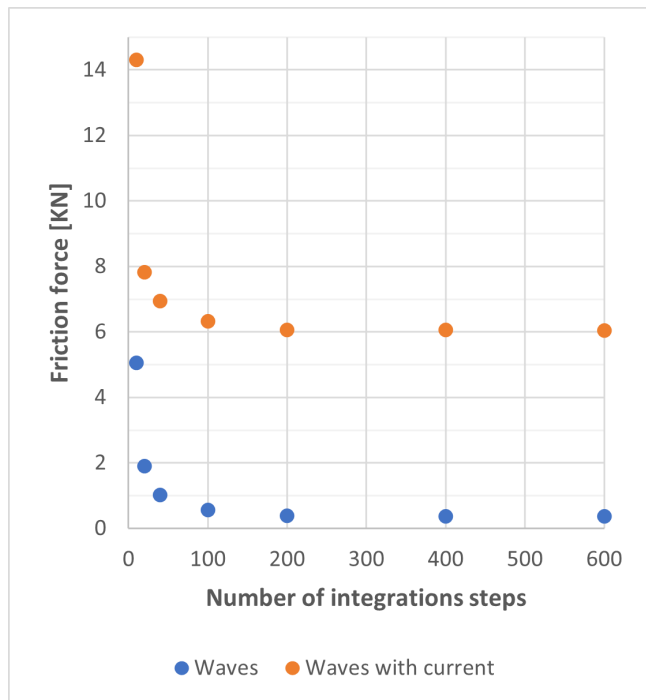


Figure 4.14: Integration steps Ocean Sun

The total friction force of the waves for the island can be seen in Figure 4.15. The maximum force is then found as the highest absolute point of the graph and is 0.364kN.

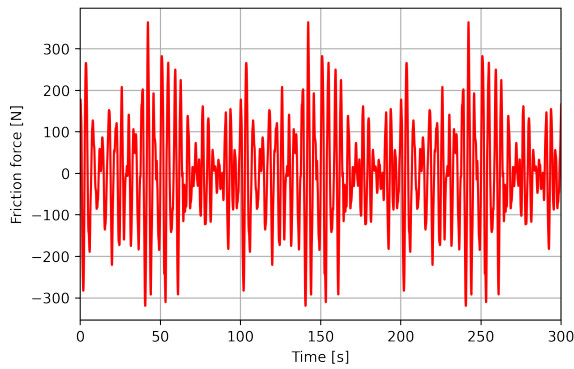


Figure 4.15: Friction force only waves

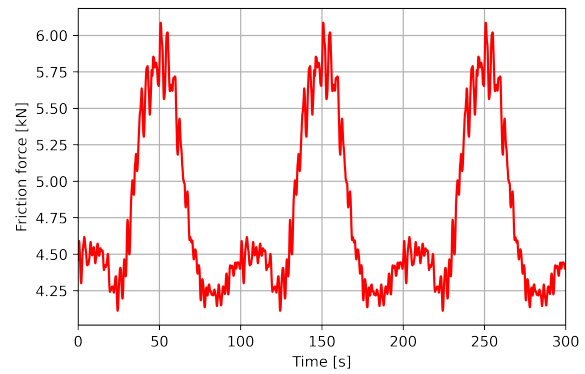


Figure 4.16: Friction force waves with current

Waves with current

For the tubes, the current can be added to the waves in a similar way as for the *Floating Solar* structure to the Morison equation as explained in subsection 4.4.4. This gives a load on the tubes for the combination of waves and current per meter of 955N and for the total island 108kN.

For the friction force, the same steps as for only the waves are taken, with the only addition that the current velocity is added to the x-component of the waves-velocity. The maximum friction force of the waves with the current is 6.05kN for the island. In Figure 4.16 it can be seen that the locations of the peaks match the peaks of Figure 4.15. The current amplifies the peaks of the friction force due to only the waves on the membrane, increasing the total loads.

	Tubes (+railing) per meter [N/m]	Tubes (+railing) island [kN]	Friction island [kN]	Total per ha [kN]	Order of magnitude [N]
Wind	139	15.7	1.23	41.7	10^5
Current	31.5	3.57	2.75	15.5	10^4
Waves	640	12.1	0.36	30.6	10^5
Waves +current	1068	19.6	6.05	63.0	10^5
Total maximum mooring load	1207	35.3	7.28	105	10^5

Table 4.4: Environmental loads Ocean Sun (72m diameter) system.

4.6. ZimFloat

The next structure is called ZimFloat and is produced by the German company Zimmermann. In the Netherlands, this system is also known as Groenleven, which is the only Dutch supplier of the system. The concept is quite similar to the *Floating Solar* system, where the panels are placed on floaters using a metal frame. The Zimfloat system is built up of multiple 'boats', where each boat consists of four square floaters, a metal frame and two rows of six panels in a rooftop shape, see Figure 4.17. The floater is approximated by a square block with rounded corners with a ratio of $r/D=0.1$ and has a drag coefficient of $C_d=1.5$ [43].



Figure 4.17: ZimFloat structure

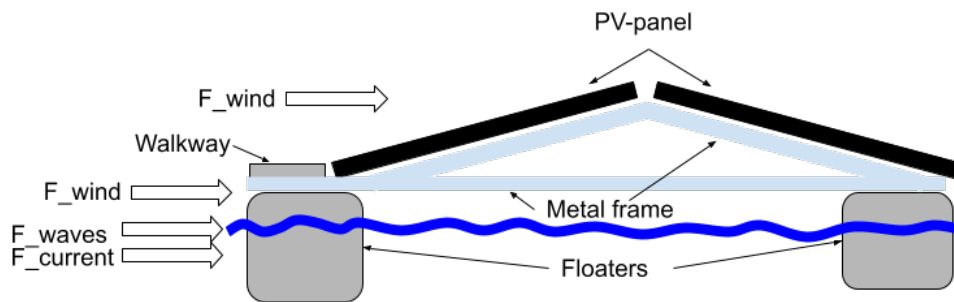


Figure 4.18: Schematic image of ZimFloat structure

4.6.1. Wind force

The wind will act on the floaters and on the PV panels. The panels are mounted with a tilt angle of 10 degrees resulting in a C_d value for the panels of 0.3, see Table 3.1. The wind force is first calculated for the panel on the left side of Figure 4.18. Exact data for the C_d value for the second panel is not available, some studies show the aerodynamic benefits of an East-West orientation [44][45]. Therefore the assumption is made that every second panel (the right one in the schematic image) only has 10% of the load of the left panel. To account for the sheltering effect of the wind on the next boats, the same sheltering factors are used as were used for the *Floating Solar* structure. The second boat has 40% of the wind load of the first boat and rows three and further downwind will have a wind load of 15%, see assumption 7. The wind load on the floaters is calculated as a force per unit length. However, the floaters do not cover the total length of the boat. Each boat with a length of 8.1 m has two rows of two floaters with a length of 2.7 m. Therefore the force is divided by the length of the boat and multiplied by two times the length of the floaters to have an average force per unit length of the boat, see Equation 4.17.

$$F_{\text{wind per meter}} = F_{\text{on floaters}} * \frac{2 * L_{\text{floater}}}{L_{\text{boat}}} \quad (4.17)$$

4.6.2. Current force

The current force for the ZimFloat structure can be found in the same way as for the *Floating Solar* structure. Only now the drag coefficient for the square floaters with rounded corners should be used ($C_d = 1.5$). And similar to the wind on the floater the force has to be scaled by the ratio of floaters per length. The shielding factor for the current can be found using Equation 3.5 where now $C_d = 1.5$, $D = 0.6$ m and $\Delta X = 5.1$ m giving a shielding factor for the current of $Sh_{\text{current}} = 0.385$.

4.6.3. Wave force

The wave force for the Zimfloat structure can be found in the same way as for the *Floating Solar* structure, using the drag coefficient found for the current. And again for finding the waves forces with

the current included in the waves, the current velocity is added to the horizontal velocity of the waves. For finding the wave forces (and waves with current) on one hectare, the local wave forces are found on each floater simultaneously and added to find the total force. The result of all forces of the Zimfloat structure can be seen in Table 4.5.

	1 section [N/m]	1ha [kN]	Order of magnitude [N]
Wind	215	116	10^5
Current	63.5	102	10^5
Waves	1371	605	10^6
Waves + current	1615	1063	10^6
Total mooring load	1830	1179	10^6

Table 4.5: Environmental loads Zimfloat system.

4.7. Overview of environmental loads

An overview of the environmental loads per structure can be found in Table 4.6 and made visual in Figure 4.19. In the graph, the contributions of the wind, current and wave loads of each structure can be seen. The combination of the waves and the current results in a force that is higher than the sum of the waves and the current. This additional force is shown as a separate category in the graph and is found by subtracting the force of only the waves and only the current from the force of the combination of the waves with the current.

	Floating Solar	Zimfloat	Ocean Sun
Wind	215	116	41.7
Current	77.1	102	15.5
Waves	163	605	30.6
Waves with current	462	1063	63.0
Total mooring load	677	1176	105

Table 4.6: Environmental loads per system for 1 hectare in [kN].

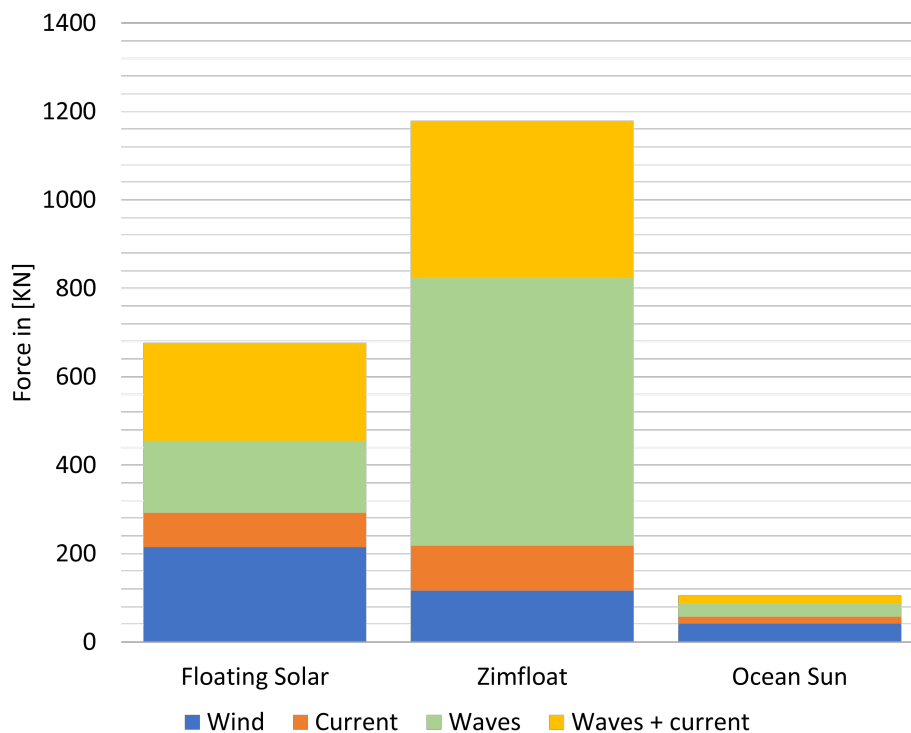


Figure 4.19: Overview environmental loads per system

The large differences in the height of these forces can be seen in [Figure 4.19](#), the membrane structure of OceanSun, designed to minimise the environmental loads, has the lowest total force of the three structures. The total mooring load for OceanSun is just 15% of that for the *Floating Solar* structure and only 9% of the ZimFloat system.

5

Multi-Criteria Analyses (MCA)

Numerous factors must be taken into consideration when deciding on the type of floating PV-system to be installed on a body of water. The variations between these systems can be high, and many new technologies have been developed in recent years. Making a well-founded decision can be challenging, and it should not rely solely on a single criterion or perspective. The decision should include criteria that are not easily quantifiable or comparable. Therefore, a decision tool in the form of a Multi Criteria Analysis (for short MCA) has been developed. An MCA is a systematic method that considers all criteria and their respective importance.

This MCA can be used in the early stages of project development to determine which types of structures are suitable for a specific location and which are not. The complete MCA is presented in [Table 5.9](#) and the values used to assign points to each structure can be found in [Appendix C](#). In this version of the matrix, all weight factors have the standard value, which later will be changed to meet the site conditions of the location. In this chapter, the decision tool including the way scores and the weight factors are determined are explained.

Ultimately, the MCA will offer a clear overview of the performance of different systems based on all relevant criteria. The system with the highest overall score is the most suitable, whereas a very low score suggests that a system should not be considered for that location.

5.1. Criteria:

The selection criteria used and how a score is given are described below for all points. More information about the criteria can be found in [section 2.2](#). For all criteria points, a higher score means that the concept performs better for those criteria. For some criteria, it is possible to set clear boundaries on how to receive a certain score. However, there are also factors that are more difficult to quantify. For these factors, the score is built up of individual features that each contribute to a point.

Environmental loads

The scores in this category are based on the calculations described in [chapter 4](#). The wind, wave and current loads are all extrapolated to a reference area of one hectare (100m by 100m). Note that for these calculations the environmental conditions found for the case-study Haringvliet are used. For all loads holds that a low force is better for the system and will therefore receive a high score. The boundaries for each criteria can be seen in [Table 5.1](#).

Score	1	2	3	4	5
Wind	>1000	1000-500	500-250	250-100	<100
Current	>1000	1000-500	500-250	250-100	<100
Waves	>2000	2000-1000	1000-500	500-200	<200

Table 5.1: Boundaries for environmental criteria in kN

System specific criteria

The boundaries for the criteria self-cleaning, marine life and T.R.L. are presented in [Table 5.2](#). For self-cleaning, a higher tilt angle will give a better score for this criteria. A lower cover ratio will increase the percentage of light that reaches the water and will increase the score. For the technical readiness level, the number of existing projects is used as a measurement for the score. The number of existing

projects per system supplier is dependent on the water category. In this way, a supplier that only operates on sill water does not receive a high score for offshore locations. This makes the matrix a dynamic table depending on the water category. The scores per water category can be seen in [Table 5.8](#). If a supplier receives a score of 0 for the T.R.L. this system is not suitable and should not be considered for this location. The other criteria in this category score points for features that the system has and are stated in [Table 5.3](#).

Points	1	2	3	4	5
Self cleaning (tilt angle [°])	0	0-5	5-15	15-25	>25
Ecological impact (1 - cover ratio [%])	0	0-15	15-30	30-45	>45
T.R.L.	no pilots yet	only pilot projects	first projects in operation	multiple projects in operation	many >MW projects

Table 5.2: Boundaries for system-specific criteria

Safety	Maintenance	Installation
Walkways included	boat access point	Shape adjustable to site
Safety railing included	All panels accessible for maintenance	Size (capacity) precisely adjustable
No significant movement due to walking	Modular build system	Uses standard available materials
Cables and lines covered or protected	No tracking system	Assembled at shoreline
Non-slip surfaces	Standard PV-panels	recyclable materials

Table 5.3: Features that score a point

Cost of energy-related criteria

The boundaries for the criteria energy density, radiation and capex are presented in [Table 5.5](#). The current maximum energy density is around 2 MPw/Ha using standard mono-crystalline panels (400 Wp with an area of $2m^2$) when placed flat without any space in between the panels. For all structures, the capacity that can be installed on an area of 1 hectare is calculated using the installed capacity and sizes of existing (pilot) projects. A high energy density results in a high score. Flexible membranes or other flat systems score significantly higher in this criteria because there is almost no space needed between the solar panels.

In order to find the exact full-load hours per system software such as PV-syst can be used. Unfortunately due to a lack of time, this was not possible in this research. Therefore an estimation of the full load hours is made depending on the orientation of the panels, see [Table 5.4](#). This estimation is made after meetings with different FPV suppliers and based on full-load hours of ground-mounted solar panels. The capex prices are given per installed capacity as EUR/Wp. As a reference, the current average capex price for ground-mounted PV is around €0.50 per Wp.

Orientation	Horizontal	East-West	South	Single axis tracking	Dual axis tracking
Full load hours	850 - 900	900 - 950	950 - 1000	1000-1050	>1050

Table 5.4: Full load hours per orientation of the PV-panels

Points	1	2	3	4	5
Energy density (Mwp/Ha)	<0,9	0.9-1.2	1.2-1.5	1.5-1.8	>1.8
Radiation (hours/year)	850-900	900-950	950-1000	1000-1050	>1050
capex (Eur/Wp)	>1.0	1.0-0.8	0.8-0.7	0.7-0.6	<0.6

Table 5.5: Boundaries for cost of energy criteria

limitations

The criteria anchoring & mooring and ice & snow are not taken into account in the multi-criteria matrix. What kind of mooring system to choose is extremely site-specific. The anchoring and mooring selection itself requires an extra detailed study after a system is chosen for a location. Therefore rating each system on their mooring system is not possible within the scope of this research.

The exact forces and reactions of ice and snow are very dependent on the location and the structure. This would unfortunately cost too much time to investigate and therefore this criteria is left out of the scope of this research.

5.2. Weight factor

Not all criteria are of equal importance in the MCA. Therefore each criteria has a weight factor. The weight factors vary from 1 to 5 and the most important criteria have the highest weights. For each concept the score per criteria is multiplied by that weight factor and all the scores are summed. In order to account for the difference in the number of criteria per category, the values of the system category are multiplied by 0.75 so each category weights evenly. The weight factors depend on the location of the site and are very important for the MCA. Before the MCA can be filled in, detailed research on the location has to be carried out. The research should identify the environmental conditions, local regulations and other development requirements. The height of the weight factors should be assigned after this research in order to use the MCA for a specific location. How to value each weight factor is described below.

5.2.1. How to determine the weight factors

The criteria are divided into three groups. Criteria that rely on the type of water, location-dependent and location-independent factors.

Weight factors that depend on the type of water

The first step is to find in what kind of water category the site is. The different types of water can be divided into four categories:

1. Still standing water with almost no waves, no current and sheltered from the wind. Examples are water basins, ponds or very small inland lakes.
2. Water with occasional waves and low current. Wind speeds can be relatively high, however, the fetch distance is limited. This category holds for inland lakes and small rivers.
3. Inland waters with high waves, currents and wind speeds. The IJsselmeer or other large lakes and the Waddenzee belong to this category.
4. Offshore waters. Unlimited fetch length with extremely high waves, current en wind speeds.

There are four criteria of which the weight factor depends on the water category. These are the environmental loads (wind, waves and current) and the capex. A higher water category means higher environmental loads and therefore these criteria are more important and will receive higher weight factors in the matrix. For the capex, a higher water category will result in a lower weight factor. This is because the competition between suppliers is high at low water categories and there is less competition for offshore suppliers. Therefore the price differences between suppliers are less important for rough waters. The weight factors for these criteria are listed in [Table 5.6](#).

Water:	Cat. 1	Cat. 2	Cat. 3	Cat. 4
Wind	3	4	5	5
Current	0	1	2	4
Waves	1	2	4	5
Capex	5	4	2	1

Table 5.6: *Weight factors that depend on the water category.*

Location-dependent

The location-dependent criteria start with the base weight factor of 3, which can be increased or decreased by one or two points when the location has certain characteristics. The self-cleaning effect

of the panels is more important for locations where high levels of birds, salt spray or dust are common and for locations where manual cleaning is difficult.

For the ecological impact of the FPV park, two distinctions have been made depending on the ecological value, and the water depth. If the ecological value is high the weight factor should be increased by a point, this is the case for ecologically protected areas such as the Natura 2000 areas. If there is no ecological value the weight factor should be decreased by a point, for example when the water is already contaminated at a dredging depot. The presence of aquatic plants depends on whether the water depth is deeper or less than 4 meters. Therefore the weight factor increases for shallow water (<4m) and decreases for deep water (>4m).

The weight factor for the technical readiness level (T.R.L.) does not directly depend on the location, however, it depends on the investor or initiator of the project. If all risks should be minimized or if this project will function as an example project for new leads it is beneficial to select a supplier that already has a proven track record and will increase the weight factor. On the other hand, if it is a pilot project or the investor values and wants to stimulate innovations in the field, the T.R.L. is less important.

The energy density (area used per installed capacity) is very important for locations where the available space is limited, and therefore the weight factor will increase. For locations where there is unlimited space available, for example offshore, the energy density is less important and the weight factor will decrease.

These criteria with the corresponding factors can be seen in [Table 5.7](#).

	+1	+1	-1	-1
Self-cleaning	difficult to reach for manual cleaning. (e.g. oceans or remote locations)	high level of birds, salt spray or dust	almost no birds in area	very easy to clean manually (e.g. small ponds with bank access)
Ecological impact	natura 2000 or other protected location	shallow water <4m	deep water >4m	no ecological value (dredging depot or drink water basin)
T.R.L.	risk-averse investor	example project for new leads	pilot project	investor values innovation
Energy density	limited space	-	unlimited space (e.g. offshore)	-

Table 5.7: Weight factors that depend on location characteristics.

Location-independent

The location-independent criteria are safety, maintenance, installation and full load hours. These criteria are all important for the decision matrix, without the weight changing per location. The safety, maintenance and installations form a group that together has a weight factor of three, each having a weight factor of one. The full-load hour has a standard weight factor of three.

5.3. Deal breakers

Certain FPV systems face physical limitations, where it is simply impossible to place a structure on a location due to the design of the structure. There are three so-called deal breakers added to the decision matrix. The first one takes into account the submerged depth of the structures and whether the structure can handle if the water body dries up. For example, the draft of the SolarDuck system is around six meters, so using this system would only be possible when the water depth is more than six meters. The second deal breaker is regarding the cover ratio. For some locations, there can be a strict limit for the minimum amount of sunlight that is able to reach the water. So for these locations, membrane-type structures are not allowed. Note that it may be possible to create open spaces between two islands in order to comply with the limit. However, there are no regulations on this subject yet. The last deal breaker focuses on the technical readiness level. If a system is not designed for a water category meaning there are not even pilot projects coming, the T.R.L. scores a 0. Each system that has a 0 for the T.R.L. is not suitable for this location.

5.4. MCA without a location

The total matrix without a location defined is shown in [Table 5.9](#). Here the weight factors are the standard value of 3, except for safety, maintenance and installation which together have a score of

3. The matrix is presented as a static table without a water category and therefore the score here is based on the overall T.R.L. of the supplier. This overall score is given in [Table 5.8](#) as water category 0.

Water cat.	Ciel & Terre (HYDRELIO)	Groenleven (Zim float)	Floating Solar	SolarDuck	Oceans of energy	Ocean Sun
1	5	5	4	0	1	1
2	1	2	3	1	1	4
3	0	1	1	2	2	5
4	0	0	0	3	3	4
0	4	4	4	2	2	4

Table 5.8: T.R.L. scores for each supplier depending on the water category.

Category	Weight (1-5)		HDPE floaters			Cylindrical floaters		Flexible structures	
	Criteria		Ciel & Terre (HYDRELIO)*	Zim float (Groenleven)	Floating Solar	SolarDuck*	Oceans of energy*	Ocean-Sun	
Environmental loads	Wind	3	4	4	4	3	5	5	
	Current	3	4	4	4	5	4	5	5
	Waves	3	3	2	3	3	4	5	5
System	Self cleaning	3	3	3	5	3	1	1	1
	Ecological impact	3	2	3	5	4	1	1	1
	T.R.L.	3	4	4	4	4	2	2	4
	Safety	1	2	3	3	3	5	1	2
	Maintenance	1	3	3	5	4	4	2	4
	Installation	1	4	4	5	3	1	3	5
	Energy density	3	3	3	5	2	3	3	4
Financial	Full load hours	3	3	2	4	2	1	1	1
	CAPEX	3	4	3	3	4	1	1	4
	Total	30	90	92.25	105	78.75	73.5	93.75	

Table 5.9: Multi criteria analyses without a location. *For these systems the loads are not calculated, but estimated based on similarities with other structures

6

Case study: Haringvliet

This chapter contains a case study with the goal of finding what kind of FPV structure is the most suitable to be installed at location Haringvliet. After an introduction of the location, the site conditions found at Haringvliet are described. Then the weight factors are determined in order to fill in the multi-criteria analyses. With the filled-in matrix, the conclusion is made about which system is the most suitable for this location.

6.1. Introduction

Haringvliet used to be connected to the North Sea until a dam was built as part of the Delta works in 1970. This former estuary still has occasionally rough storms with high wind speeds and waves. The location Haringvliet is selected by Ventolines as a new place to generate renewable energy on water. This will be accomplished by placing solar panels on floaters and thereby creating a floating solar park. The location is chosen for two main reasons. The first one is that there is already a windpark of five turbines with a capacity of 20MW located at the northern shore of the Haringvliet. This is beneficial due to the option to share the existing electrical cables. When the wind blows, the sun often doesn't shine. And when the sun shines, the wind usually does not blow. Wind and solar parks that are close to each other can therefore easily be connected to the same cable, also known as cable pooling. The second reason for choosing this location is because the rougher water conditions and the ecological value can serve as a stepping stone towards realising floating solar on the IJsselmeer. This project can be used to learn what the waves will do to a floating structure and what steps are crucial in obtaining the permits for ecologically protected areas.

6.2. Site conditions:

The site conditions found in this section provide the input parameters and other relevant factors that are needed in the development phase of an FPV project.

6.2.1. Location

The location chosen for the FPV system is at Haringvliet in the province of Zuid-Holland. The coordinates of the location are 51.72N, 4.39E and the site has a surface area of 31.1ha. It is located at the North-west side of the Haringvlietbridge and can be seen in [Figure 6.1](#). The area can be approximated by a rectangular of roughly 1500m by 200m.



Figure 6.1: Location Haringvliet

6.2.2. Wind

Wind data is provided by the KNMI (Koninklijk Nederlands Meteorologisch Instituut) which has multiple weather stations in the Netherlands [46]. The station at Stavenisse is the closest one to Haringvliet and is approximately 30km in the south-west direction. The location of the weather station can be seen in Figure 6.2 where the black dot is the FPV-location at Haringvliet and the red dot is the location of the KNMI measuring station. Daily measurements are available for the past 25 years. This data contains the daily and hourly maximum average wind speeds, wind directions, strongest wind gusts and some more data that is not needed for this research.

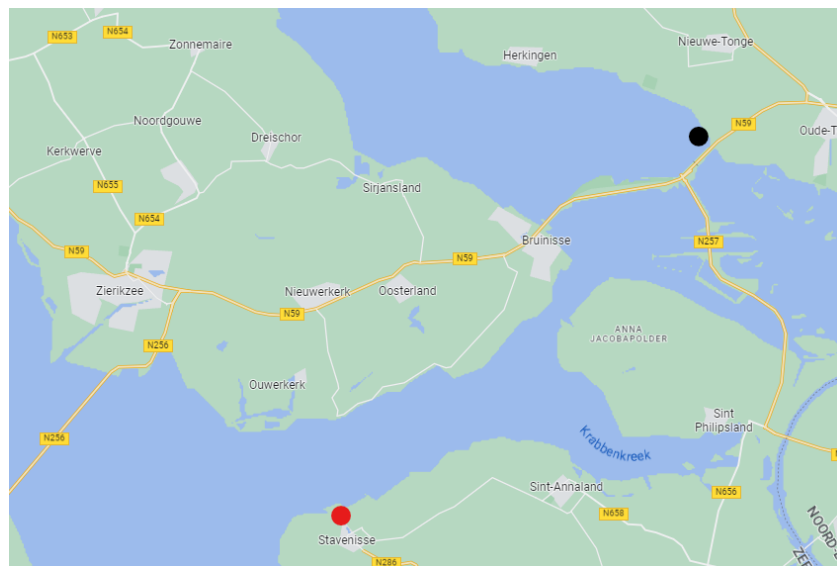


Figure 6.2: Location of KNMI measuring station (red dot).

Wind-speed

All wind speeds from the KNMI are measured at (or corrected to) a reference height of 10m. The solar panels will be placed in a range between 0 and 2m above the water surface depending on what kind of structure is chosen. The actual wind speed at 1m height will be lower than measured at the reference height of 10m. This wind speed can be calculated using Equation 3.3, which is repeated below.

$$U(h) = U(h_{ref}) \frac{\ln\left(\frac{h}{z_0}\right)}{\ln\left(\frac{h_{ref}}{z_0}\right)} \quad (6.1)$$

$$U(1m) = U(10m) * 0.7297$$

Where U is the wind-speed, $z_0 = 0.002m$ for water surfaces, $h = 1m$ and $h_{ref} = 10m$.

The average wind speed at Stavenisse over the past 25 years measured by the KNMI is $5.54 \frac{m}{s}$, adjusted to 1m height gives $4.04 \frac{m}{s}$.

The operational lifetime of this project is approximately 25 years. It is necessary to perform an extreme value analysis in order to predict the maximum expected wind speed in the coming years. For this project, a return period of 50 years is chosen. This means that the calculated value is expected to occur once every 50 years. This method is an estimation of a natural phenomenon that can be unpredictable. Therefore a safety factor is needed and the return period is significantly larger than the lifetime of the structure.

The KNMI data is divided into yearly segments and for each year a maximum hourly average wind speed was found. These values are converted to match a height of 1m and then sorted in ascending order. The yearly maxima are plotted with years of recurrence on the x-axis with a logarithmic scale and wind speed on the y-axis. Subsequently, a straight line is fitted through the data points and extrapolated to 50 years. The wind speed found at the intersection of the fitted line and the line $x=50$ years is the wind speed with a 50-year return period. As can be seen in Figure 6.3 the expected maximum hourly wind speed for 50 years is $20.1 \frac{m}{s}$. Exactly the same method is used to evaluate the maximum wind gust and the daily average wind speed with a return period of 50 years. The wind-gust plot can be seen in Figure 6.4 and has a value of $30.3 \frac{m}{s}$. The maximum daily average windspeed with a 50-year return period is $13.6 \frac{m}{s}$.

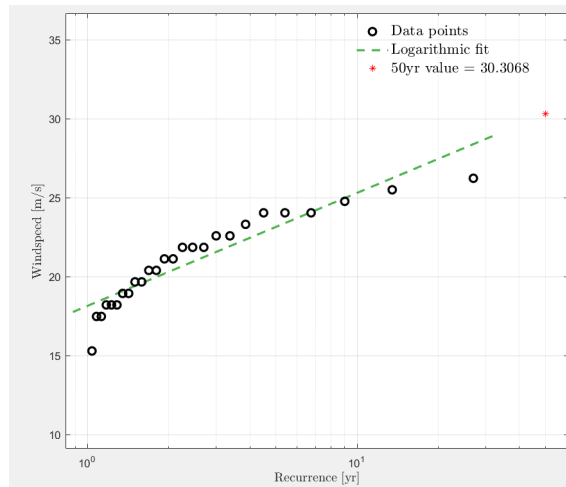
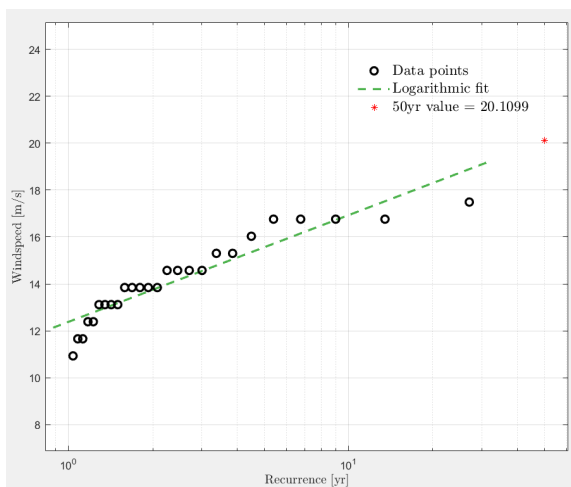


Figure 6.3: 50-year extreme value hourly windspeed **Figure 6.4:** 50-year extreme value maximum windgust

	V_{10}	V_1
Average windspeed	5.54	4.04
50 years maximum wind gust	41.2	30.3
50 years maximum hourly windspeed	27.5	20.1
50 years maximum daily windspeed	18.6	13.6

Table 6.1: Windspeed at reference height and at 1m, all in [m/s]

Wind direction

The direction of the wind is given in degrees with respect to true north. Calculating the average wind direction directly for the data can give false information because the wind direction at 359 degrees is almost the same as 0 degrees which are both north. Small variations here can lead to a large error in

finding the average wind direction. To easily visualise the most common wind directions a windrose is made and can be found in Figure 6.5. In a windrose, the directions of the wind and the distribution of the wind speeds can be easily seen. The windrose shows that the average and in this case the most common wind direction measured by the KNMI at Stavenisse in the last 25 years is in the South-West direction.

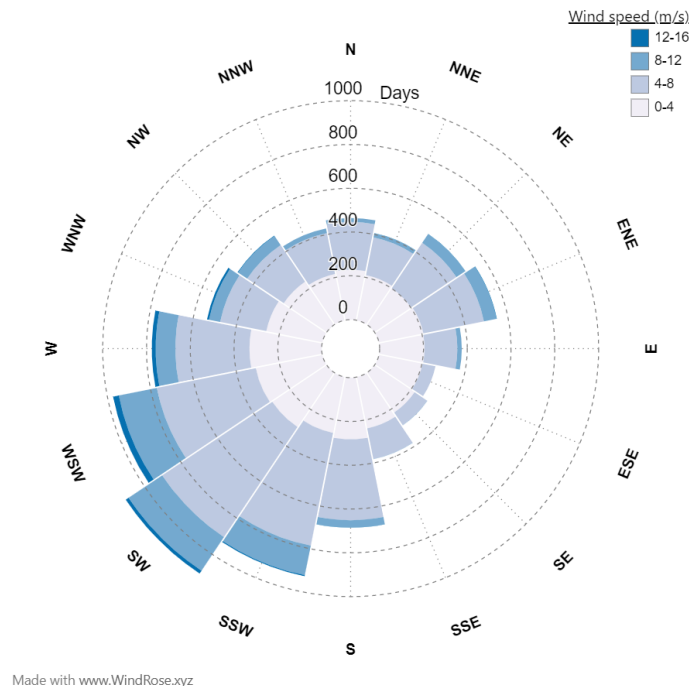


Figure 6.5: Windrose from the KNMI data at Stavenisse

6.2.3. Bathymetry

The area is located near the bank on the north side of the Haringvliet. According to data received from Rijkswaterstaat, the depth ranges from 0.1m below NAP near the river bank to 8.2m below NAP further from shore. Navionics [47] is a tool for ships to navigate that provides a map with depth lines shown in Figure 6.6. This data gives depth lines from 1m near shore with 6.4m as the deepest point which comes close to the data given by Rijkswaterstaat. The increase in depth is 6.4m over a length over 200m which is an average slope of 3.2%.

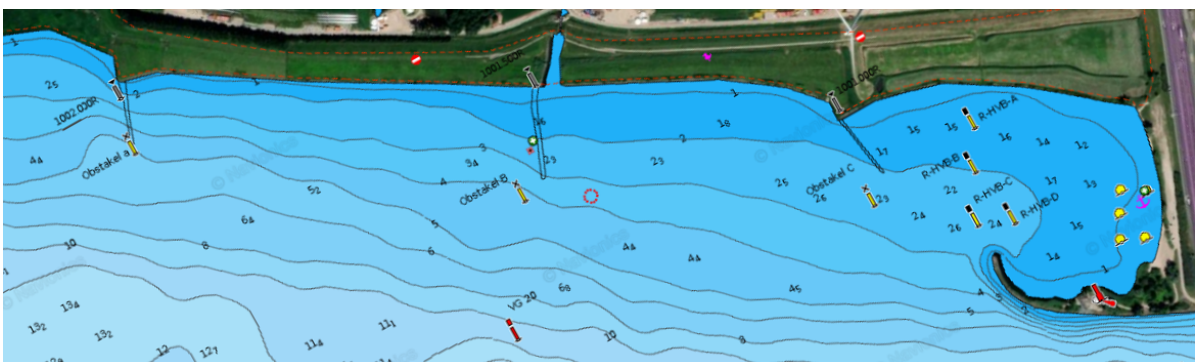


Figure 6.6: Depth-lines [47]

6.2.4. Soil composition

Information about the soil can be needed for the placement of anchors and the attachment of mooring lines. The soil composition can be split up in two parts, namely the soil underwater at the riverbed and the soil onshore at the riverbank. For the soil at the riverbed, data is provided by the research institute TNO commissioned by the Dutch government and available on www.DINOloket.nl [48]. The drill sample is taken approximately 500m to the south of the chosen location. For the soil at the

riverbank, data is provided by the Ministry of the Interior and Kingdom Relations and available on www.BROloket.nl [49]. This drill sample is taken on the bank on the west side of the Haringvlietbridge. In [Table 6.2](#) and [Table 6.3](#) the materials of the different soil layers and the vertical limits with respect to ground level are given. For the exact locations of the drill samples see [Appendix B](#).

Layer	upper limit [m]	lower limit [m]	material / description
1	0.00	-4.45	sand (very fine), silty
2	-4.45	-5.10	sand (very fine), clayey
3	-5.10	-6.20	clay
4	-6.20	-6.80	sand (very fine), clayey
5	-6.80	-10.90	clay
6	-10.90	-11.50	sand (very fine), clayey

Table 6.2: Soil composition riverbed

Layer	upper limit [m]	lower limit [m]	material / description
1	0.00	-0.55	clay, sandy clay
2	-0.55	-1.00	sand
4	-1.00	-1.70	peat

Table 6.3: Soil composition riverbank

6.2.5. Waves

In the Netherlands, Rijkswaterstaat is responsible for the construction, management and maintenance of all rivers. They continuously measure water height, currents and tides with measuring buoys and this data is freely accessible [50]. Unfortunately, the buoy at the Haringvlietbridge does not provide any data about the height, length or frequencies of the waves. After contact Rijkswaterstaat specified that waves up to 1m occur during stormy weather from experience but unfortunately had no data to support that claim. Therefore an estimation of the waves has to be computed with the local wind speed, fetch and depth.

Fetch

As mentioned before, the fetch is the free distance over which the wind can blow to generate waves. Normally this is the distance from the shore to the desired location. However, at the location Haringvliet there are multiple very shallow parts that limit the maximum fetch distance. These shallow areas will limit the growth of the waves or can cause the waves to break. The shallow part right next to the island Tiengemeten and the sandbank Ventjagersplaat can be seen [Figure 6.7](#). Taking these shallow areas into account, the maximum fetch for location Haringvliet is approximately 3 kilometres.



Figure 6.7: Maximum fetch distance [47]

Waves caused by wind

The fetch is the limiting factor for the waves assuming the wind will blow constantly for a day at the highest daily average of $18.6 \frac{m}{s}$ at a reference height of 10 meters, given in [Table 6.1](#).

Deep water conditions

Assuming deep water conditions the significant wave height can be determined with the fetch and the windspeed using the relation from [subsection 3.3.1](#). Using these equations the estimated value of $H_{max} = 1.4m$ in [Equation 6.2](#) can be assumed to be the maximum expected wave height in 50 years for waves generated by the wind when assuming deep water.

$$\begin{aligned}\tilde{F} &= \frac{g * F}{U_{10}^2} = \frac{9.81 * 3000}{18.6^2} = 84.7 \\ \tilde{H} &= 0.24 * [\tanh(4.41e^{-4} * \tilde{F}^{0.79})]^{0.572} = 0.021 \\ H_s &= \frac{U_{10}^2 * \tilde{H}}{g} = \frac{18.6^2 * 0.021}{9.81} = 0.761m \\ H_{max} &\approx 2 * H_s = 2 * 0.761 = 1.52m\end{aligned}\tag{6.2}$$

$$\begin{aligned}\tilde{T} &= 7.69 * [\tanh(2.77e^{-7} * \tilde{F}^{1.45})]^{0.187} = 1.52 \\ T_p &= \frac{U_{10} * \tilde{T}}{g} = \frac{18.6 * 1.52}{9.81} = 2.89s\end{aligned}\tag{6.3}$$

In the calculations above the assumption is made that the location can be considered as deep water. For deep water conditions to be valid the water depth must be larger than half the wavelength. For the Haringvliet river, the water depth over the fetch varies between 0 and 13 meters. With the highest depths occurring only in the fairways and water depths till 6 meters in between the fairways. The wavelength can be found using the dispersion relationship, see [Equation 3.8](#). Using the period calculated above and an average water depth of 5 meters, the wavelength will be 12.8 meters. With this wavelength, the minimum water depth is 6.35 meters in order to have deep water conditions. Therefore for most parts of the Haringvliet, the deep water conditions do not apply and a shallow water estimation for the waves has to be used.

Shallow water spectrum

For the location at Haringvliet, a model is needed that takes the limited water depth into account. For shallow water, a TMA (Texel-Marsen-Arsole) spectrum can be used. In this spectrum, a factor is added so the influence of the finite water depth is included. The factor ϕ depends on the frequency and the water depth. The model of Bouws et al. (1985) [35] added the extra factor to the Jonswap spectrum, and this spectrum is given in [Equation 6.4](#).

$$E(f) = \frac{\alpha * g^2}{(2\pi)^4 * f^5} \exp\left[-\frac{5}{4} \left(\frac{f}{f_p}\right)^{-4}\right] * \gamma^{\exp\left[\frac{-(f-f_p)^2}{2 * \sigma^2 * f_p^2}\right]} * \phi(2\pi f, h)\tag{6.4}$$

where:

$$\begin{aligned}\alpha &= 0.0078 \left[\frac{2\pi * V_{10}^2}{g * L_p} \right]^{0.49} \\ \gamma &= 2.47 \left[\frac{2\pi * V_{10}^2}{g * L_p} \right]^{0.39} \\ \phi(2\pi f, h) &= \omega_h^2 / 2 \text{ for } \omega_h \leq 1 \\ \phi(2\pi f, h) &= 1 - 0.5 * (2 - \omega_h)^2 \text{ for } \omega_h > 1 \\ \sigma &= 0.07 \text{ for } f \leq f_p \\ \sigma &= 0.09 \text{ for } f > f_p \\ f_p &= \frac{3.5 * g}{V_{10}} \left[\frac{g * F}{V_{10}^2} \right]^{-0.33} = \text{Peak frequency} \\ L_p &= \text{Wavelength corresponding to } f_p\end{aligned}$$

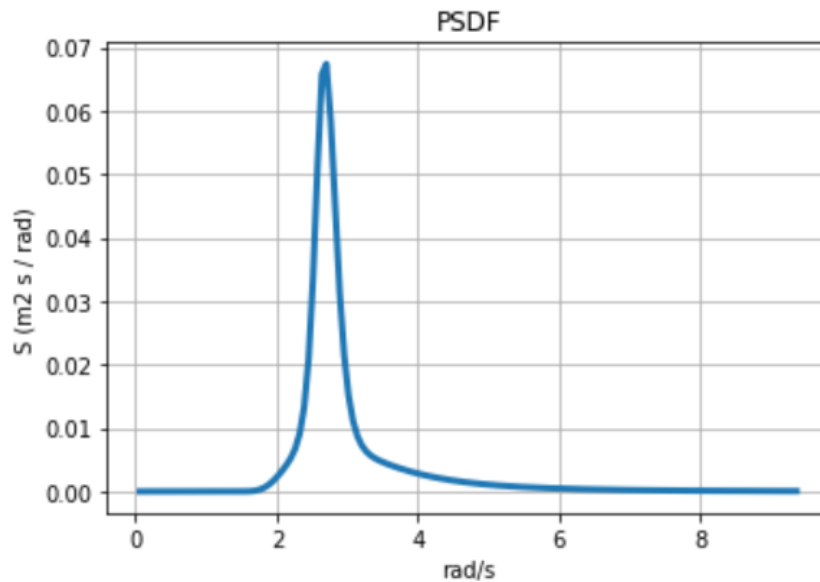


Figure 6.8: Power spectral density function of TMA-spectrum

For the location in the Haringvliet, a windspeed of $V_{10} = 18.6 \frac{m}{s}$ (see Figure 6.2.2) and an average depth of $d = 5m$ is used to get the spectrum given in Figure 6.8. The significant wave height (H_S) can be found using this spectrum with the relation that $H_S = 4 * \sqrt{m_0}$. Where m_0 is the variance of the spectrum and is equal to the surface under the PSDF plot. The significant wave height using the shallow water spectrum is $H_S = 0.751m$. With this wave spectrum, a time-series of the elevation, velocity and acceleration can be generated. A part of the total elevation profile is given in Figure 6.9, The velocity and acceleration profiles can be seen in Appendix B

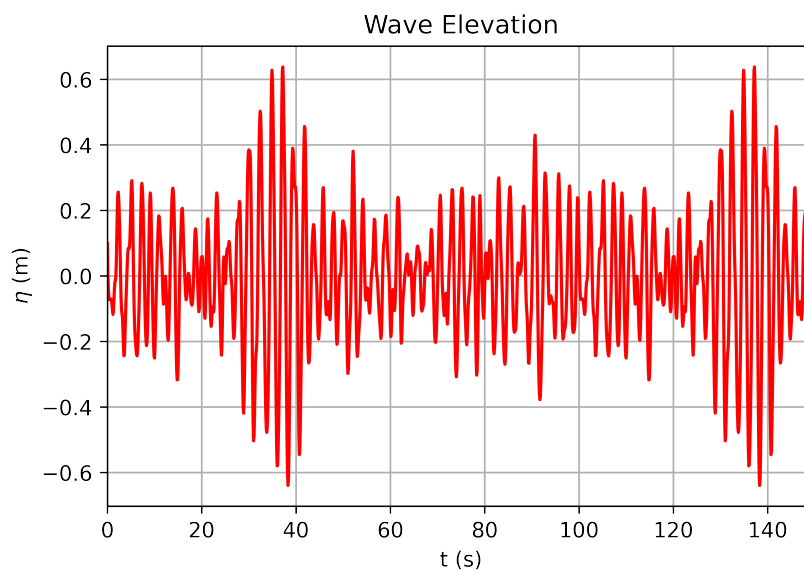


Figure 6.9: Wave elevation profile

Waves caused by ships

Next to the wind waves, waves can also be caused by ships that are passing by. These ships can be split up into two categories. The first one is commercial ships such as freight ships and dredging ships. The number of freight ships passing by is limited because most ships coming from Hollandsch Diep are heading South to Volkerak and do not enter the Haringvliet. The second category is for pleasure and are mainly smaller sail- and speedboats. The commercial ships are often very large with a high draft so they are limited by the fairway that can be seen in Figure 6.10. Pleasure ships are less limited to the fairway, however, according to Rijkswaterstaat the water depth can be very unpredictable due to sludge accumulations. Therefore it can be assumed that all ships with a minimum draft will follow the

dredged fairway. This fairway is only 100 meters away from the site and therefore the waves produced by the ships can have a negative effect on the floating structure. Unfortunately, no information can be found on the height of the waves caused by the ships and due to a lack of time the waves caused by ships are not further investigated.

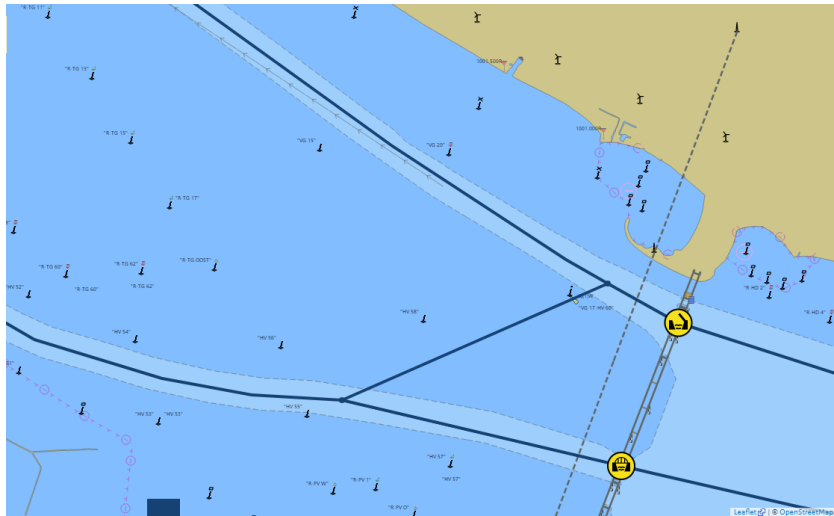


Figure 6.10: Fairway and location bridge [51]

6.2.6. Tides

Rijkswaterstaat has a measurement buoy at 'Rak noord' approximately 3.5km to the southeast that provides data on the water level. In this data clear fluctuations per day and month are visible. The average daily tides have an amplitude of 15cm. The extreme values are measured at -4cm for the lowest point and 170cm for the highest point with respect to NAP (Normaal Amsterdams Peil, Dutch standard where 0 is approximately equivalent to sea level). The tides are important for the mooring system, allowing the structure to move vertically while keeping it in place. However, the mooring structure is not within the scope of this research.

6.2.7. Current

The buoy at the Haringvlietbridge mentioned in subsection 6.2.5 has measured the current between January 2008 and June 2010. The current is given as a magnitude without a direction, however, the natural flow of the river is from East to West. In this 2.5 years, the current is measured every minute with some exceptions where data is missing and a value of 1E38 was given. The average current over these 2.5 years is very low with a value of only $0.09 \frac{m}{s}$. The current reaches a few times per year a value higher than $0.4 \frac{m}{s}$ and the maximum peak measured is $0.65 \frac{m}{s}$. The site is located just behind a small protrusion, which will lower the currents. The exact effect is unknown and therefore the $0.65 \frac{m}{s}$ is taken as the maximum expected current.

6.2.8. Natura 2000

Nature 2000 is a European network of protected areas with the goal of maintaining biodiversity by providing a natural environment for flora and fauna [52]. Almost all water areas in the Netherlands are part of the Natura 2000 network. The location at Haringvliet is a Natura 2000 area which results in stricter environmental rules. The materials that are used may not have a negative influence on the water quality. There is a maximum cover ratio, the ratio between the total area and the area blocked for sunlight, in order to maintain a healthy under-water environment. These rules have a high influence on the design choices and play a big role in obtaining the permits.

6.3. Decision matrix

6.3.1. Weight factors

As described in section 5.2 the weight factors depend on the location and the site conditions. Having all the site conditions the height of each weight factor can be determined. The first step is to find what kind of water category the location Haringvliet is. The wind speed can be high and the current is relatively low due to the dam at the end of the river. The maximum wave height is limited due to a

relatively short fetch of three kilometres. Therefore the roughness of the water is category two, this means that the weight factors for the environmental loads and the capex can be found in [Table 5.6](#). The site is located in an area where a large number of birds can be expected, due to the nature reserve a the nearby island Tiengemeten. It is not a very remote location, nor is it accessible without a boat, the self-cleaning criteria score a weight factor of 4. The ecological impact has a weight factor of 5 because it is in a protected area called Natura 2000 and the water depth is less than 4 meters for a large part of the site. A part of the function of this project is to learn and show the capabilities of Ventolines for new projects, without it being a pilot project. Therefore the T.R.L. scores a weight factor of 4. The location has an area of 31 hectares, which limits the maximum capacity of the projects, the weight for the energy density is increased by a point. The rest of the criteria are not site dependent and all score the standard points, an overview of all weights for the location Haringvliet can be seen in [Table 6.4](#).

Criteria	Weight (1-5)	Note
Wind	4	Cat. 2
Waves	2	Cat. 2
Current	1	Cat. 2
Self cleaning	4	Birds, not remote nor easily accessible
Ecological impact	5	Natura 2000, and large part <4m
T.R.L.	4	Example project
Safety	1	Standard 1
Maintenance	1	Standard 1
Installation	1	Standard 1
Energy density	4	Limited space
Full load hours	3	Standard 3
CAPEX	4	Cat. 2

Table 6.4: Weight factors Haringvliet

6.3.2. Filled in matrix

Category	Criteria	Weight (1-5)	HDPE floaters			Cylindrical floaters	Flexible structures
			Ciel & Terre (HYDRELIO)*	Zim float (Groenleven)	Floating Solar		
Environmental loads	Wind	4	4	4	4	3	5
	Current	1	4	4	5	4	5
	Waves	2	3	2	3	4	5
System	Self cleaning	4	3	3	5	3	1
	Ecological impact	5	2	3	5	4	1
	T.R.L.	4	1	2	3	1	4
	Safety	1	2	3	3	5	1
	Maintenance	1	3	5	4	4	2
	Installation	1	4	5	3	1	3
	Energy density	4	3	5	2	3	3
Financial	Full load hours	3	3	2	4	2	1
	CAPEX	4	4	3	4	1	4
	Total	34	89.25	98	113.25	80.5	68.25

Table 6.5: Filled in matrix for Haringvliet. *For these systems the loads are not calculated, but estimated based on similarities with other structures

6.3.3. Results

As can be seen in [Table 6.5](#) the system with the highest score of 113.25 points is *Floating Solar*. Their system performs relatively well for the environmental loads and scores high for the self-cleaning and ecological impact. With a relatively large gap, the second best is for the Zimfloat system with 98 points and a close third for the OceanSun system with 97 points. The flexible structures score very well on the environmental criteria, however, due to the full cover ratio and horizontally orientated panels they miss many points in criteria that are highly valued for this location. SolarDuck and Oceans of Energy have the lowest scores and are therefore less suitable for this location. The system of SolarDuck is marked red, due to one of the deal breakers mentioned in [section 5.3](#). The water depth of the site a Haringvliet is for the largest part less than 6 meters, resulting that the SolarDuck system can not be placed there.

7

Discussion

7.1. Environmental loads

In [chapter 4](#) the environmental loads for the systems *Floating Solar*, *Zimfloat* en *OceanSun* are calculated with as input factors the environmental conditions found at location Haringvliet. For each system, the wind, wave, current, current included in the waves and the total mooring loads are found. For all structures, the current has the lowest contribution to the total force. For the *Zimfloat* system, the wind is the second highest and the waves make the largest contribution to the total load. For *Floating Solar* and *OceanSun* holds that the wind load is higher than the force of only the waves, but that the combination of the waves and current is higher than the wind load.

The *Oceansun* system is designed in a way that minimises the surface area above the waterline for the wind load and also below the waterline for the current and wave loads. The wind load of the *Floating Solar* structure is higher than that of the *Zimfloat* structure. This is because the panels in the *Zimfloat* structure are oriented in a rooftop shape with a smaller tilt angle which makes the system closer to the water and more aerodynamic than the *Floating Solar* structure. For the waves load the *Zimfloat* structure has by far the highest forces, this is because the square floaters of the *Zimfloat* structure have a much larger volume than the circular tubes of *Floating Solar* which increases the inertia component of the wave forces. The different shapes of the structures complicate the consistency in the calculation of the forces, they are adjusted to fit the corresponding structure. For example, the friction forces are only found for the large horizontal surface of the *OceanSun* membrane and not for the other two structures.

In the calculations, the assumption is made that the structures do not affect the waves. However in reality the structures will interact with the waves and will have a damping effect resulting in lower wave forces for part of the structures that are behind other parts. The *OceanSun* membrane is designed to move along with the waves, this movement can result in extra surface areas on which the wind of waves can act which has not been investigated in the research.

When assessing the forces resulting from the interaction of waves and currents, as well as determining the overall mooring load, the assumption is made that the directions of wind, waves, and current are all aligned. This approach ensures a worst-case scenario, finding the maximum potential loads on the structures. However in reality the wind and wind-generated waves approach primarily from the South-West, while the current predominantly flows seaward in an East-to-West direction. Therefore assuming that all the forces act on the structure from the same direction and at the same time is a conservative assumption. Furthermore, the assumption of a zero-degree angle of attack implies that all forces act perpendicularly to the front of the structure. Research shows that this results in the highest loads. Nevertheless, conducting an analysis that takes into account multiple angles of attack and different combinations of wind, waves, and current directions would give a more accurate representation of the actual conditions.

Furthermore, only wind-generated waves are taken into account when finding the environmental loads. Other loads such as waves caused by ships, accidental loads due to collisions or snow and ice loads are not taken into account in the scope of this research.

7.2. Multi criteria matrix

The multi-criteria matrix shows a clear overview of the different systems and on which criteria they perform well or not. The matrix can be used as a tool for helping to select what type of floating PV structure is best suitable for a given location when the site conditions of that location are known. Without the selection of a location, the system of *Floating Solar* has the highest score, than the Zimfloat system and in third place the OceanSun membrane. The system of Oceans has the lowest score, this can be explained because their system is, with only pilot projects, still in the development phase and because it is designed for offshore the prices are higher.

The validity of the matrix should be checked if the conditions differ greatly from those on the Haringvliet. This is because the environmental loads are computed with input parameters that belong to the Haringvliet. New environmental loads can be found for a new location using the methods of this thesis and the new input parameters form the new location.

Not all possible factors are taken into account in the matrix. For example, whether the system can withstand the site running dry, mandatory maintenance contracts and additional loads due to snow and ice. Other factors can play a role in the decision that are not directly related to the design of the system. Examples are the country of origin of the supplier, ways of working, availability of the system, or previous encounters with the suppliers. Therefore the matrix should be used as a tool that can help with the selection of a system and not as a black box that makes the decision itself.

Because floating PV is still a growing and relatively new field, there are constant improvements in the designs and new systems are being developed. The information on which the matrix is made and the calculations are based all come from data that was available in 2023, therefore it is needed that the matrix is updated and expended when new designs appear.

7.3. Case study Haringvliet

The filled-in matrix for Haringvliet shows that the system of *Floating Solar* is the best option, followed after a large gap by Zimfloat and the OceanSun system. The full cover ratio of the OceanSun membrane could reduce the chance of obtaining a permit due to ecological concerns. The system of SolarDuck is designed for offshore environments with deep water. The draft of the floaters is six meters, meaning that the structure would only be possible at a small part of the site near the fairway. The case study Haringvliet shows the complexity of finding the environmental conditions for a site if detailed measurements are not available. The wind data is taken from a location nearby, that provides a good estimation of the wind speeds. It would be better if wind measurements were performed at the exact location of the FPV park. The current is measured at the Haringvlietbridge, the site is located behind the Haringvliet Bridge on the north side. On the east side of the project area, this has created a lee zone where the current velocities would be lower. The wave data is generated from the wind speed, water depth and the fetch distance for the 50-year highest daily wind velocity. This is an estimation of the waves and real-time wave data measured by a buoy would give more accurate results.

The significant wave height found for the location at the maximum wind velocity is 0.75 meters. The concept with the highest score, the *Floating Solar* system, can only guarantee structural integrity with waves up to 0.55 meters. Therefore it is probably needed to install some kind of (floating) wave breaker. This wave breaker will dampen the waves and can also function as a protection from boats or other materials that can cause collisions with the FPV-park.

8

Conclusions

In this chapter, the research questions that were given in [section 1.2](#) are answered and conclusions following this research are given. Before the main research question is answered the following sub-questions are answered first.

Sub-question 1:

Which criteria are the most important for the selection of a floating PV structure?

The selection of an FPV structure involves many important criteria. These criteria and their importance depend on the site conditions of the desired location. Important factors can be split up into three categories. The first is the environmental loads, containing the force due to the wind, waves and current. The second category is about system-dependent features, this category focuses on the ecological impact, ease of maintenance, reliability and safety of the structure. The last category is about the financial aspects of the system and contains besides the costs, also the energy yield of the system. All these criteria are important for an FPV structure that should be analysed when selecting a system.

Sub-question 2:

What are the wind, waves and current loads on different FPV structures?

The wind, wave and current loads on an FPV structure are site-specific and time-dependent. To answer this question the maximum expected loads are calculated for multiple systems at a single location. The location chosen for these calculations is the case study Haringvliet. The result shows that for all systems the current has the smallest impact with forces in the order of magnitude ranging from 10^4 to 10^5 Newton. The wind has a slightly higher impact on the structures and is in the order of magnitude of 10^5 Newton. The highest loads are found for the waves ranging from 10^4 Newton for the OceanSun to 10^6 Newton for the Zimfloat structure.

The differences between the structures are large with the OceanSun system having by far the lowest overall mooring load of only $1.1 * 10^5$ N. The *Floating Solar* structure has a total mooring force of more than six times a high of $6.7 * 10^5$ N and the Zimfloat system has the highest overall load with a magnitude of $1.2 * 10^6$ N.

Case study:

Sub-question 3a:

What are the environmental site conditions for the Haringvliet location?

The site conditions at Haringvliet show that due to the closing of the estuary with the North Sea, the current velocities are low. The wind with the predominant direction from the southwest has a relatively large open area before reaching the location. For the waves no measured data was available, the maximum expected waves are found using the wind speed, water depth and maximum fetch distance. This gives a maximum significant wave height of 0.75 meters and waves up to 1.5 meters.

Sub-question 3:

Which existing floating PV structure is the most suitable for the rougher inland water conditions at Haringvliet?

With the environmental loads of the location, the weight factors of the matrix are adjusted. This gives a clear overview of the structures and shows that the system of *Floating Solar* is the best option for this location. The Zimfloat structure follows with only a few less points. The structures of SolarDuck and Oceans of Energy are both not suitable to be placed at Haringvliet.

Main research question:

How to determine which floating-PV technology to select for a specific location in a preliminary phase of project development? In this thesis, a decision tool is created that uses a multi-criteria analysis that is adaptable to a specific location by the use of weight factors. The outcome is a matrix where scores are assigned to multiple important aspects for six different kinds of FPV structures. After a study of the environmental conditions for the desired location, the tool can then be used to find out which of the structures are suitable and interesting for further research and which structures are not suitable for that location and can be ruled out for further consideration.

9

Recommendations

9.1. For future research

In this thesis, the maximum loads are found that will act on the structures. However, this does not provide any information on whether these structures are capable of withstanding these loads. New research is needed that determines the maximum forces a system can handle and what kind of fatigue occurs in the lifetime of 25 years.

For FPV parks that are installed in waters where ships are present, the waves caused by these ships can introduce additional forces acting on the FPV structure. The magnitude of these forces can have a significant effect on the structures, especially frequent waves that can lead to fatigue loads. More research is needed to find out what is impact of these waves is. It could also be interesting to identify and analyse accidental limit states such as collisions, extreme drought or vandalism.

The calculations are only performed for three of the six systems in the multi-criteria matrix and the scores of the other structure are based on estimations. It would be interesting to analyse the exact forces on these structures to increase the accuracy of the matrix. In order to keep the matrix relevant, new systems should be added to the matrix and the current systems should be updated whenever changes are made in the design.

9.2. For Ventolines

The first recommendation for Ventolines is to start with measuring wave elevations for all new locations, as soon as possible. This can easily be done by placing measurement buoys in the desired location and will provide clear data that can be used to analyse the forces. The method used in this thesis where the waves are estimated by the wind will only give an estimation of the waves, measuring the waves will give a more realistic image of the waves and forces.

The outcome of the case study shows that the system of *Floating Solar* is the best option to install at Haringvliet. However, the waves at Haringvliet are higher than the maximum wave height given by *Floating Solar*. Therefore it would probably be necessary to install a breakwater around the FPV park. The effect of this breakwater should be analysed in future research.

Bibliography

- [1] Rijksoverheid. klimaatbeleid, February 2023. URL <https://www.rijksoverheid.nl/onderwerpen/klimaatverandering/klimaatbeleid>.
- [2] Rijksoverheid. Duurzame energie, February 2023. URL <https://www.rijksoverheid.nl/onderwerpen/duurzame-energie>.
- [3] Centraal bureau voor de statistiek. Aandeel hernieuwbare energie in 2022 toegenomen naar 15 procent, September 2023. URL <https://www.cbs.nl/nl-nl/nieuws/2023/22/aandeel-hernieuwbare-energie-in-2022-toegenomen-naar-15-procent#:~:text=Aandeel%20hernieuwbare%20energie%20in%202022%20toegenomen%20naar%2015%20procent,-2%2D6%2D2023&text=Het%20verbruik%20van%20hernieuwbare%20energie,en%20het%20laagst%20sinds%201990>.
- [4] Rijksoverheid. Offshore wind energy, April 2023. URL <https://www.government.nl/topics/renewable-energy/offshore-wind-energy>.
- [5] Rijksoverheid. Rijksoverheid stimuleert gebruik aardwarmte, April 2023. URL <https://www.rijksoverheid.nl/onderwerpen/duurzame-energie/aardwarmte>.
- [6] Raniero Cazzaniga and Marco Rosa-Clot. The booming of floating PV. *Solar Energy*, 219: 3–10, May 2021. doi:[10.1016/j.solener.2020.09.057](https://doi.org/10.1016/j.solener.2020.09.057). URL <https://doi.org/10.1016/j.solener.2020.09.057>.
- [7] Haohui Liu, Abhishek Kumar, and Thomas Reindl. The dawn of floating solar—technology, benefits, and challenges. In *Lecture Notes in Civil Engineering*, pages 373–383. Springer Singapore, July 2019. doi:[10.1007/978-981-13-8743-2_21](https://doi.org/10.1007/978-981-13-8743-2_21). URL https://doi.org/10.1007/978-981-13-8743-2_21.
- [8] Matti Kummu, Hans de Moel, Philip J. Ward, and Olli Varis. How close do we live to water? a global analysis of population distance to freshwater bodies. *PLoS ONE*, 6(6): e20578, June 2011. doi:[10.1371/journal.pone.0020578](https://doi.org/10.1371/journal.pone.0020578). URL <https://doi.org/10.1371/journal.pone.0020578>.
- [9] ESMAP World Bank Group and SERIS. Where sun meets water floating solar handbook for practitioners. *World Bank*, 2019. URL https://www.seris.nus.edu.sg/doc/publications/ESMAP_FloatingSolar_Gde_A4%20WEBL-REV2.pdf.
- [10] Kim Trapani and Miguel Redón Santafé. A review of floating photovoltaic installations: 2007-2013. *Progress in Photovoltaics: Research and Applications*, 23(4):524–532, January 2014. doi:[10.1002/pip.2466](https://doi.org/10.1002/pip.2466). URL <https://doi.org/10.1002/pip.2466>.
- [11] Yubin Jin, Shijie Hu, Alan D. Ziegler, Luke Gibson, J. Elliott Campbell, Rongrong Xu, Deliang Chen, Kai Zhu, Yan Zheng, Bin Ye, Fan Ye, and Zhenzhong Zeng. Energy production and water savings from floating solar photovoltaics on global reservoirs. *Nature Sustainability*, March 2023. doi:[10.1038/s41893-023-01089-6](https://doi.org/10.1038/s41893-023-01089-6). URL <https://doi.org/10.1038/s41893-023-01089-6>.
- [12] Yousuf, Zahid, Khokhar. A Review on Floating Photovoltaic Technology (FPVT). *Current Photovoltaic Research*, August 2020. URL https://www.researchgate.net/publication/347818468_A_Review_on_Floating_Solar_Photovoltaic_Power_Plants.
- [13] : Simon Tonnel, Maria Ikhennicheu, Richard Le Failler, Felix Gorintin, Umberto Varbaro, Alba Alcañiz Moya, and Hesam Ziar. Guidelines for design, procurement and o&m friendly concepts for floating pv, 2023.
- [14] Ciel et Terre. Floating solar, January 2023. URL <https://ciel-et-terre.net/>.

- [15] Sungrow floating. TO BE THE RELIABLE FPV SYSTEM & SOLUTION SUPPLIER, February 2023. URL <https://uk.sungrowpower.com/SolutionsDetail/1088>.
- [16] Oceans of Energy. Oceans of Energy, Januari 2023. URL <https://oceansofenergy.blue/north-sea-1/>.
- [17] SolarDuck. Solarduck, Januari 2023. URL <https://solarduck.tech/unique-solution/>.
- [18] Bluewater. Renewable energy solutions, February 2023. URL <https://www.bluewater.com/our-solutions/renewable-energy-solutions/>.
- [19] Zimmermann PV-Floating. ZIM Float – Floating PV System, February 2023. URL <https://pv-floating.com/>.
- [20] FloatingSolar. Proef toont aan: Drijvende panelen Floating Solar zijn stormbestendig, February 2023. URL <https://www.floatingsolar.nl/proef-toont-aan-drijvende-panelen-floating-solar-zijn-stormbestendig/>.
- [21] FloatingSolar. FloatingSolar, February 2023. URL <https://www.floatingsolar.nl/ons-product/>.
- [22] OceanSun. OceanSun, Januari 2023. URL <https://oceansun.no/the-innovation/>.
- [23] Kim Trapani, Dean L. Millar, and Helen C.M. Smith. Novel offshore application of photovoltaics in comparison to conventional marine renewable energy technologies. *Renewable Energy*, 50:879–888, February 2013. doi:[10.1016/j.renene.2012.08.043](https://doi.org/10.1016/j.renene.2012.08.043). URL <https://doi.org/10.1016/j.renene.2012.08.043>.
- [24] EUROPEAN STANDARD. Actions on structures - Part 1-3: General actions - Snow loads. *Eurocode 1*, Part 1-3:, March 2004.
- [25] S.K Chakrabarti. *Hydrodynamics of offshore structures*. Computational Mechanics Publications, 1987.
- [26] Seok Min Choi, Chang-Dae Park, Sung-Hoon Cho, and Byung-Ju Lim. Effects of wind loads on the solar panel array of a floating photovoltaic system – experimental study and economic analysis. *Energy*, 256:124649, October 2022. doi:[10.1016/j.energy.2022.124649](https://doi.org/10.1016/j.energy.2022.124649). URL <https://doi.org/10.1016/j.energy.2022.124649>.
- [27] Seok Min Choi, Ga Ram Lee, Chang Dae Park, Sung Hoon Cho, and Byung Ju Lim. Wind load on the solar panel array of a floating photovoltaic system under extreme hurricane conditions. *Sustainable Energy Technologies and Assessments*, 48:101616, December 2021. doi:[10.1016/j.seta.2021.101616](https://doi.org/10.1016/j.seta.2021.101616). URL <https://doi.org/10.1016/j.seta.2021.101616>.
- [28] M. Mammam, S. Djouimaa2 a, A. Hamidat1, S. Bahria1, and M. El Ganaoui. Wind effect on full-scale design of heliostat with torque tube. *Mechanics & Industry*, 2016.
- [29] Sulaiman O. Fadlallah, Timothy N. Anderson, and Roy J. Nates. Flow behaviour and aerodynamic loading on a stand-alone heliostat: wind incidence effect. *Arabian Journal for Science and Engineering*, 2021.
- [30] Imran Ismail Sheikh. Numerical investigation of drag and lift coefficient on a fixed tilt ground mounted photovoltaic module system over inclined terrain. *International Journal of Fluids Engineering*, 2019.
- [31] Simon Watson. Lecture notes offshore wind farm design lecture 5a, April 2021.
- [32] Robert D. Blevins. *Flow-Induced Vibration*. Krieger Publishing Company, 2001.
- [33] Dr. M. Tissier. Lecture notes ocean waves lecture 10, October 2020.
- [34] Stephen Bolton. Chapter thirteen - operation and maintenance. In Kurt E. Thomsen, editor, *Offshore Wind (Second Edition)*, pages 243–283. Academic Press, Boston, second edition edition, 2014. ISBN 978-0-12-410422-8. doi:<https://doi.org/10.1016/B978-0-12-410422-8.00013-3>. URL <https://www.sciencedirect.com/science/article/pii/B9780124104228000133>.

- [35] E. Bouws, H. Günther, W. Rosenthal, and C. L. Vincent. Similarity of the wind wave spectrum in finite depth water: 1. spectral form. *Journal of Geophysical Research*, 90(C1):975, 1985. doi:[10.1029/jc090ic01p00975](https://doi.org/10.1029/jc090ic01p00975). URL <https://doi.org/10.1029/jc090ic01p00975>.
- [36] J.R. Morison, J.W. Johnson, and S.A. Schaaf. The force exerted by surface waves on piles. *Journal of Petroleum Technology*, 2(05):149–154, May 1950. doi:[10.2118/950149-g](https://doi.org/10.2118/950149-g). URL <https://doi.org/10.2118/950149-g>.
- [37] John R. Chaplin. Nonlinear forces on a horizontal cylinder beneath waves. *Journal of Fluid Mechanics*, 147(-1):449, October 1984. doi:[10.1017/s0022112084002160](https://doi.org/10.1017/s0022112084002160). URL <https://doi.org/10.1017/s0022112084002160>.
- [38] Henko Engberts. conversation about the results of first calculations. Personal conversation, 2023. Floating Solar, Rhenen.
- [39] Guanghao Chen, Md. Mahbub Alam, and Yu Zhou. Dependence of added mass on cylinder cross-sectional geometry and orientation. *Journal of Fluids and Structures*, 99:103142, November 2020. doi:[10.1016/j.jfluidstructs.2020.103142](https://doi.org/10.1016/j.jfluidstructs.2020.103142). URL <https://doi.org/10.1016/j.jfluidstructs.2020.103142>.
- [40] Petter Grøn. conversation about the dimensions of oceansun structure. Personal conversation, 2023. OceanSiun, online.
- [41] J. S. Hoving. Lecture 6: Ice actions i: Limiting mechanisms, Februari 2021.
- [42] Are J. Berstad and Petter Grøn. Model basin testing of a floating solar system compared to analysis for establishment of design verification culture. *MARINE*, 2023.
- [43] Nivedan Vishwanath, Aditya K. Saravanakumar and Kush Dwivedi, Kalluri R.C. Murthy, Pardha S.Gurugubelli, and Sabareesh G. Rajasekharan. 3d numerical investigation of a rounded corner square cylinder for supercritical flows. *Wind and Structures*, 35:55–66, Nov 2021. doi:doi.org/10.12989/was.2022.35.1.055. URL <https://arxiv.org/ftp/arxiv/papers/2112/2112.00164.pdf>.
- [44] Andrea Mignone, Gabriele Inghirami, Francesco Rubini, Raniero Cazzaniga, Monica Cicu, and Marco Rosa-Clot. Numerical simulations of wind-loaded floating solar panels. *Solar Energy*, 219:42–49, May 2021. doi:[10.1016/j.solener.2020.11.079](https://doi.org/10.1016/j.solener.2020.11.079). URL <https://doi.org/10.1016/j.solener.2020.11.079>.
- [45] Pongwit Siribodhi and Phacharaporn Bunyawachakul. Study and evaluation of a solar floating traction under severe wind conditions. *IOP Conference Series: Materials Science and Engineering*, 642(1):012003, October 2019. doi:[10.1088/1757-899x/642/1/012003](https://doi.org/10.1088/1757-899x/642/1/012003). URL <https://doi.org/10.1088/1757-899x/642/1/012003>.
- [46] KNMI. Daggegevens van het weer in Nederland, December 2022. URL <https://www.knmi.nl/nederland-nu/klimatologie/daggegevens>.
- [47] Navionics, Garmin. Navionics, March 2023. URL <https://webapp.navionics.com/#boating@13&key=eduzHcbyY>.
- [48] TNO. DINOloket, February 2023. URL <https://www.dinoloket.nl/ondergrondmodellen/kaart>.
- [49] Ministry of the Interior and Kingdom Relations. BROloket, February 2023. URL <https://www.broloket.nl/ondergrondgegevens>.
- [50] Rijkswaterstaat. Waterinfo, Januari 2023. URL <https://waterinfo.rws.nl/#!/nav/index/>.
- [51] Rijkswaterstaat. Fairway, February 2023. URL <https://vaarweginformatie.nl/frp/main/#/geo/map?viewport=51.711847;4.331918;51.730218;4.414315&layers=FAIRWAY&layers=BRIDGE&sublayer=ROUTE&term=>.
- [52] Ministry of Agriculture, Nature and Food Quality. Natura 2000, February 2023. URL <https://www.natura2000.nl/>.

Appendices

A

Appendix A

Element	Description	Symbol	Value	Unit
Tubes	Diameter	T_D	0.315	m
	Thickness	T_T	0.0077	m
	Density	T_rho	960	kg/m ³
	Drag coefficient water	T_Cd_water	1.0	-
	Drag coefficient air	T_Cd_air	1.0	-
	Inertia coefficient water	T_Ci	2.0	-
Panels	Length	P_L	1.722	m
	Width	P_W	1.134	m
	Thickness	P_T	0.03	m
	Mass	P_M	20.8	kg
	Drag coefficient air	P_Cd	0.6	-
system	Tilt angle	T	30	deg
	Spacing tubes	SP	1.8	m
	Draft	Dr	0.146	m
	Shielding wind row 2	Sh_w_row2	0.4	-
	Shielding wind row >2	Sh_w	0.15	-
	Shielding current	Sh_c	0.445	-

Table A.1: Dimensions of Floating Solar system

Element	Description	Symbol	Value	Unit
Floater	Length	F_L	2.7	m
	Width	F_W	0.6	m
	Height	F_H	0.6	kg/m ³
	Drag coefficient water	T_Cd_water	1.5	-
	Drag coefficient air	T_Cd_air	1.5	-
	Inertia coefficient	F_Ci_air	2.0	-
Boat (12 panels)	Length	L_boat	8.1	m
	Width	W_boat	5	m
Panels	Length	P_L	2.5	m
	Width	P_W	1.35	m
	Thickness	P_T	0.03	m
	Drag coefficient air	P_Cd	0.3	-
system	Tilt angle	T	10	deg
	Draft	Dr	0.3	m
	Shielding wind row 2	Sh_w_row2	0.4	-
	Shielding wind row >2	Sh_w	0.15	-
	Shielding current	Sh_c	0.445	-

Table A.2: Dimensions of Zimmermann system

Element	Discription	Symbol	Value	Unit
Tubes	Diameter	T_D	0.4	m
	Thickness	T_T	0.00153	m
	Density	T_rho	960	kg/m3
	Drag coefficient water	T_Cd_water	1	-
	Drag coefficient air	T_Cd_air	1	-
Panels	Length	P_L	1.722	m
	Width	P_W	1.134	m
	Thickness	P_T	0.03	m
	Mass	P_M	20.8	kg
	Drag coefficient air	P_Cd	0	-
Railing	Height	R_H	0.8	m
	Diameter	R_D	0.14	m
	Drag coefficient air	R_CD	1.0	-
system	Tilt angle	T	0	deg
	Spacing tubes	SP	0.1	m
	Draft tubes	Dr	0.133	m
	Thickness membrane	T_mem	0.001	m
	Friction coefficients air	C_fric_air	0.002	-
	Friction coefficients water	C_fric_water	0.0032	-
	Shielding tubes water	Sh_water	0.294	-
	Shielding tubes air	Sh_air	0.1	-
	Diameter island	D_island	72	m
	Mass island	M_island	55000	kg

Table A.3: Dimensions of OceanSun (72m diameter) system

B

Appendix B

This appendix contains extra information or figures that belong to the case study location Haringvliet.

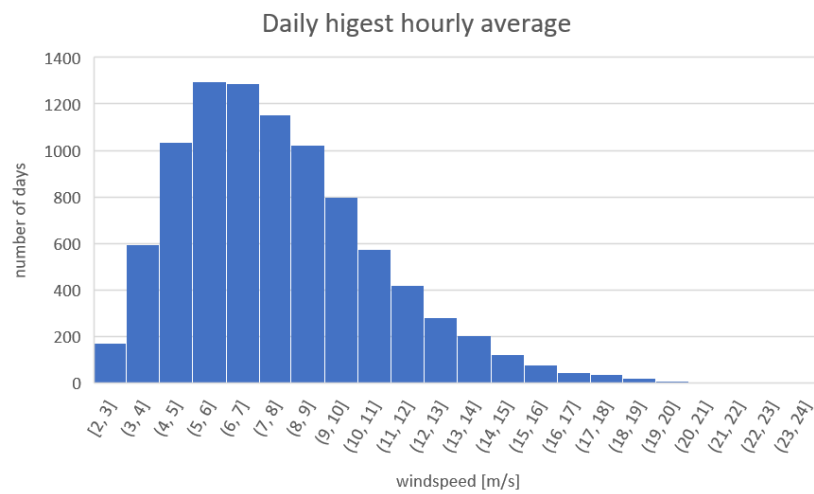


Figure B.1: Histogram of daily highest hourly average

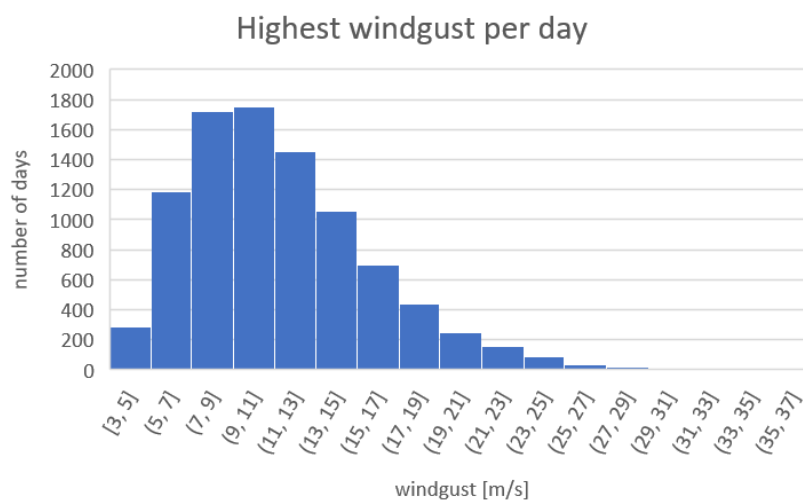


Figure B.2: Histogram of the highest daily wind-gust

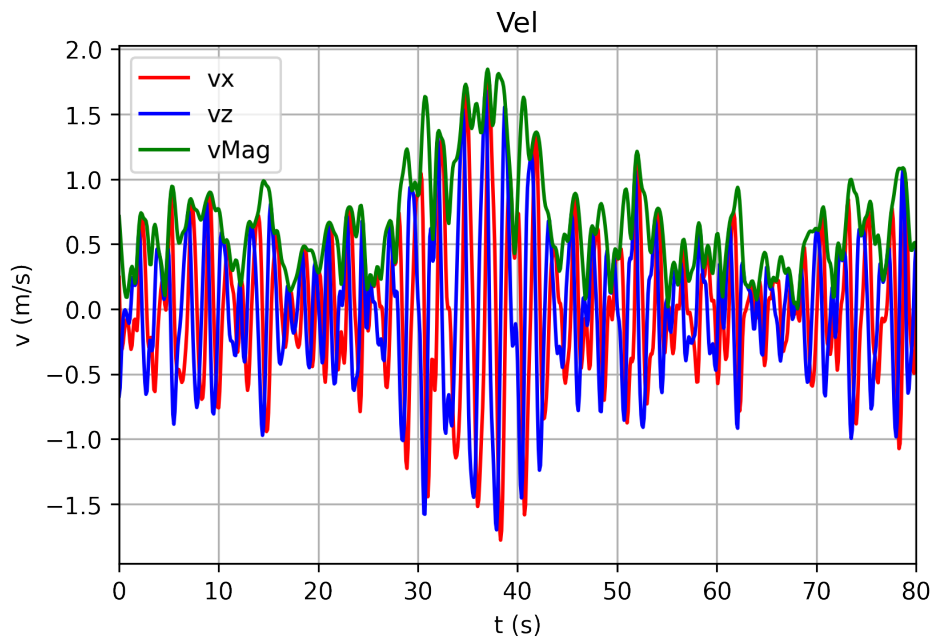


Figure B.3: Velocity of water particles

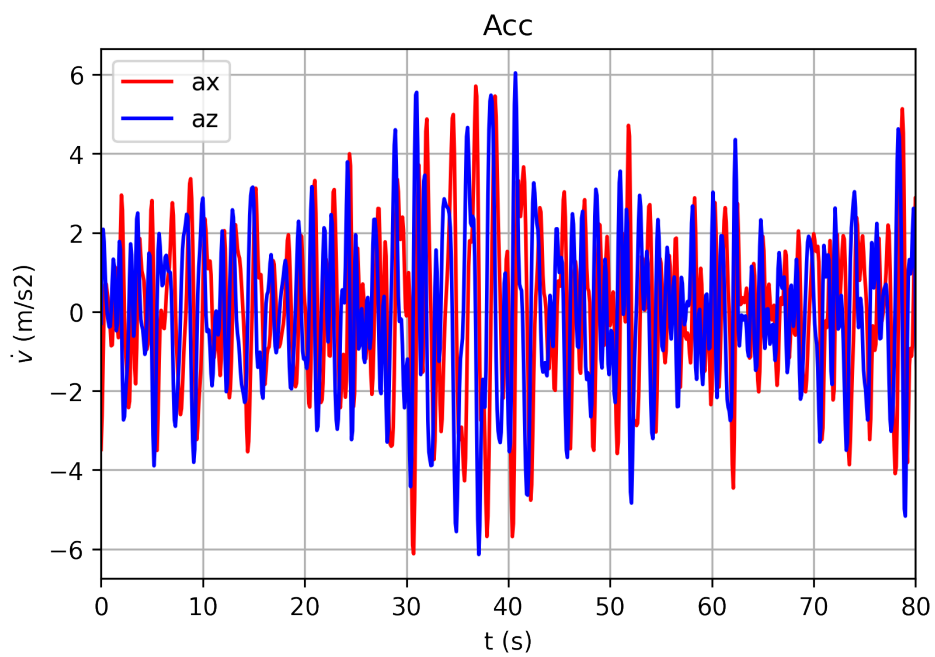


Figure B.4: Acceleration of water particles

Soil data riverbed retrieved from DINOLOket.

Boormonsterprofiel en interpretatie BRO DGM v2.2

Identificatie: B43E0158
 Coördinaten: 86184, 414839 (RD)
 Maaiveld: -3.60 m t.o.v. NAP
 Diepte t.o.v. maaiveld: 0.00 m - 11.50 m

Diepte t.o.v. maaiveld in meters

Tussen 0 en 11.5 m

Opslaan profiel

Maaiveld

Kies een ander model

BRO DGM v2.2

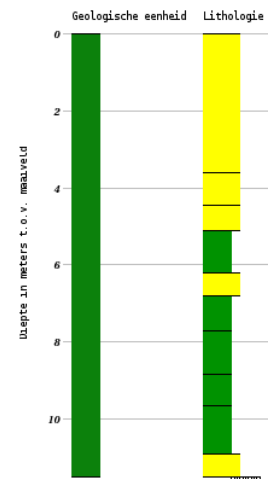
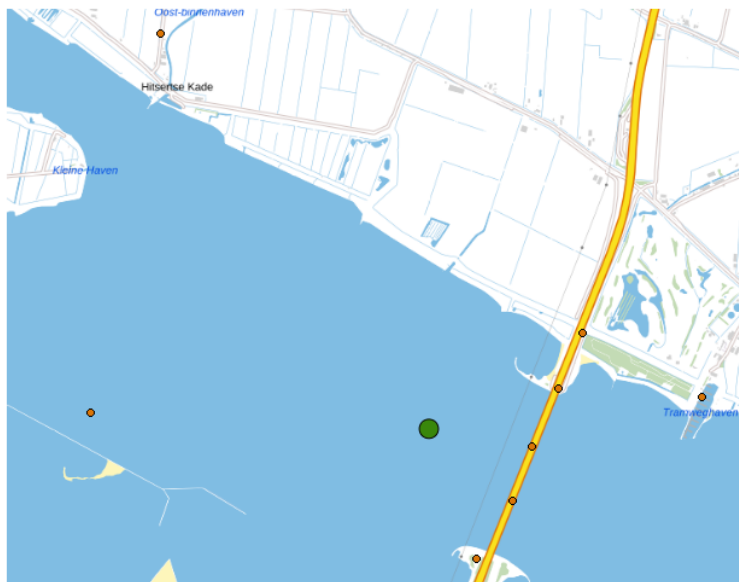


Figure B.5: location drill sample [48]

Soildata riverbank retrieved from BROloket.

Bodemkundig booronderzoek BRO

BRO-ID BHR000000102953

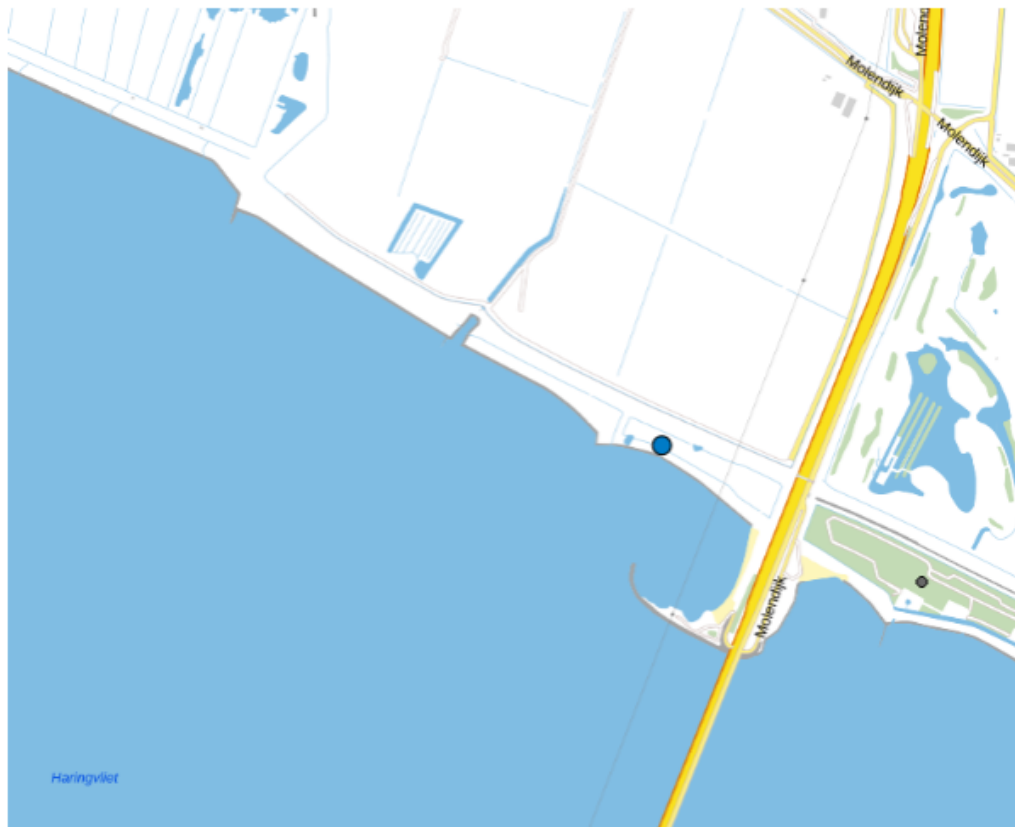


Figure B.6: location drill sample [49]

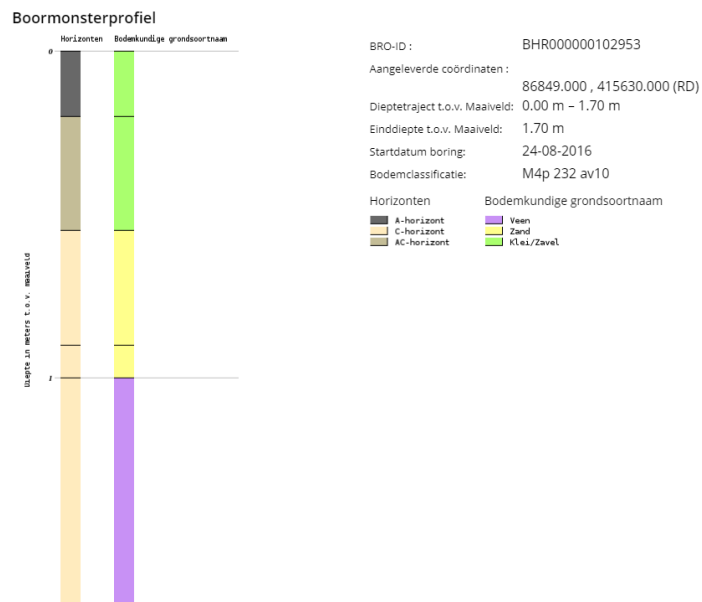


Figure B.7: drill sample [49]

C

Appendix C

Category			HDPE floaters				Cylindrical floaters	Flexible structures	
	Criteria	Unit	Ciel & Terre (HYDRELIO)*	Groenleven (Zim float)	Floating Solar	SolarDuck *		Oceans of energy*	Ocean Sun
Environmental loads	Wind	kN	250-100	116	215	500-250	<100	43.1	
	Current	kN	500-250	102	77.1	250-100	<100	16.9	
	Waves	kN	2000-500	5483	2896	2000-500	<500	174	
System	Self cleaning	Deg	10	12	30	10	0	0	
	Ecological impact	% sunlight	10	20	50.6	40	0	0	
	T.R.L.	-	many >MW project	many >MW project	multiple projects in operation	only pilot projects	only pilot projects	multiple projects in operation	
	Safety	points	2	3	4	5	1	2	
	Maintenance	points	3	5	4	4	2	4	
	Installation	points	4	5	3	1	3	5	
Financial	Energy density	MWp/Ha	1.3	1.8	1.15	1	1.67	1.47	
	Full load hours	Hours/year	950-1000	900-950	1000-1050	900-950	850-900	850-900	
	CAPEX	EUR/Wp	0.65	0.8	0.7	3	>1	0.65	

Table C.1: Values for the MCA